CHEMICAL MODIFICATION OF MESOPOROUS CARBON FOR ENERGY STORAGE APPLICATIONS

A Thesis

Presented to the Faculty of the Graduate School

of Cornell University

In Partial Fulfillment of the Requirements for the Degree of

Master of Science

by

Snatika Sarkar

August,2018

ABSTRACT

Rechargeable Lithium Sulfur batteries have attracted widespread attention due to their high theoretical energy density, which is of great importance due to growing energy demands. These batteries have not been commercialized due to the challenges caused by their complex electrochemical reactions such as the shuttle effect and solubility of higher order Polysulfides in the electrolytes. In this thesis, we discuss attempts to combat these technical issues by combining physical and chemical modifications of mesoporous carbon nanofibers as electrodes or interlayers, by incorporation of cyclic Nitrogen groups, using Gas-Assisted electrospinning and electrospraying techniques. We also compare the synergistic effects off all these features on battery performance and use various characterization tools to understand them.

BIOGRAPHICAL SKETCH

Snatika Sarkar was born in India, on March 22, 1994. She developed an interest in Science and Mathematics since her early school days. Towards the end of her High School , she decided she wanted to pursue Chemical Engineering for her career. She gained admission to the Birla Institute of Science and Technology, Pilani, as an undergraduate in Chemical Engineering for four years, followed by her Masters of Science at Cornell University. At Cornell University, she carried out independent research in the exciting field of developing next generation Lithium Sulfur batteries.

ACKNOWLEDGMENTS

I would like to thank my advisor Professor Yong L Joo for including me in this exciting project, providing me useful insights and motivating me throughout my MS research. I would also like to thank my committee member Prof. Jin Suntivich for his valuable inputs and suggestions.

I would like to extend my thanks to Dr Jin Hong Lee and the rest of the Joo group members for providing me useful training required to carry out research in energy storage.

Finally, I would like to express my gratitude to my parents for their endless love and support and for the opportunity to carry out my graduate studies at Cornell University.

TABLE OF CONTENTS

CHAPTER 1

INTRODUCTION

Lithium Sulfur Batteries: An Overview

As demand for energy increases, there is a growing need for clean, efficient and cost effective renewable energy sources and reduce the usage of fossil fuels. Lithium Sulfur batteries have a high theoretical energy density of 2600 Wh/kg and a specific capacity of 1675 mAh/g. Sulfur is abundantly available and is environmentally benign [1-3]. All these reasons make Lithium Sulfur batteries among one of the most promising next generation rechargeable batteries. However, Lithium Sulfur batteries face several challenges in performance that need to be resolved before they can be commercially viable. One of these is the dissolution of higher order polysulfides into the electrolyte, which makes it difficult to recover them as Lithium Sulfide precipitate on the cathode at the end of discharge cycle, leading to loss of active material and low capacity. Another challenge is the polysulfide shuttle effect, when the higher order polysulfides migrate to the anode, get reduced to Li2S and migrate back to the cathode to get reoxidized. The insulating nature of Sulfur and Lithium Sulfide also adds to the cell resistance [4-7].

Several efforts have been made to combat the technical issues mentioned above. It has been found that several types of carbon nanomaterials such as microporous carbon, mesoporous carbon, hierarchical porous carbon, carbon black, hollow carbon spheres, CNTs, CNFs, reduced graphene oxide and graphene can improve cell performance. These porous carbons can contain the active material, constrain the dissolved polysulfides, and accelerate charge/electron transport [8-14]. Manthiram et al introduced the concept of inserting an interlayer between the cathode and separator to acts as a polysulfide entrapper and enhance the reutilization of trapped material. However, despite the improved performance, this acts as a

temporary solution since the interlayer acts as only a physical barrier and the polysulfides can eventually leach out to the electrolyte [15]

To ensure more permanent constraining of polysulfides, chemical modification of active hosts surface are also effective in reducing shuttle effect and improving cycle performance. Introduction of doping elements like Nitrogen, Sulfur, Phosphorus, Boron have been shown formation of strong chemical bonds between the polysulfides and these elements[16,17]. Nitrogen doping has been done by introducing electron-rich functional groups like Amines, polypyrrole, pyrroles, pyridines and has been found to be effective in assisting mesoporous carbon in suppressing polysulfide shuttling effect through Lewis Acid-Base interactions with polysulfides[18-23].

Functionalizing Carbon with Nitrogen

Incorporation of Nitrogen into carbon susbtrates like Carbon Nanotubes (CNTs), Carbon Nanofibers (CNFs) has been found to be beneficial in improving electrochemical and electrocatalytic activity of Metal-ion batteries, fuel cells and super capacitors.

Wang *et al* reported the effect of addition of Nitrogen sources like Melamine, Aniline, Urea and Polyaniline to Polyacrylonitrile (PAN) precursors which were used for electrospinning [24]. Addition of these Nitrogen sources in varying ratios with respect to PAN increased the nitrogen content of the electrospun Carbon nanofibers. The diameter and morphology of the fibers was also affected as a result, due to increased viscosity of the precursors. Carbonization of the nanofibers incorporated Pyridinic and Pyrollic Nitrogen groups which resulted in significant improvement in electrocatalytic activity of fuel cells.

Xu *et al* reported a facile synthesis of highly doped CNFs for application in Potassium-ion batteries [25]. A polypyrrole precursor was prepared by oxidation of pyrrole monomers in the presence of Ammonium Persulfate reagent. The precursor was carbonized at varying temperatures to obtain CNFs doped with pyrollic Nitrogen and utilized as Anode. the resulting CNFs had a 13.8% Nitrogen content. It was found that with increasing carbonization

temperature from 650-1100^{0}C, the Nitrogen content reduced, resulting in reduction of specific capacity.

Another study by Zhang *et al*, reported the addition of urea to PAN precursors in varying concentrations for electrospinning [26]. The carbonization of the electrospun nanofibers introduced C-N and C=N bonds due to the presence of Pyridinic and Pyrollic Nitrogen groups, which increased their conductivity. The Nitrogen content increased from 11.31-19.06% with increasing Urea content from 10-30wt% in the PAN precursor. These fibers were utilized as Anode material and fibers derived from 30 wt% Urea precursors resulted in maximum improvement in electrochemical performance.

Chen *et al* reported a one step, process for N-doping multiwalled CNTs utilized as Oxidation Reduction Reaction(ORR) catalyst support [27]. Ammonium Hydroxide was used as a Nitrogen source for doping CNTs in a hydrothermal reaction at 180^{0}C for 12 hours. This synthesis has several advantages: cost effective, mild reaction conditions and also maintains the high BET surface area and original multiwalled structure of the CNTs. This method is also flexible and can be utilized for heteroatom doping of Carbon . However it results in a low Nitrogen content (1.32 at%) . Though this contributes to the improved electrocatalytic activity and durability of CNTs, this method of Nitrogen doping may not be useful for the Lithium Sulfur system used in our work.

Another interesting technique of using Polypyrrole doped carbon was reported by Guo *et al* [28]. PAN were functionalized with Polypyrrole by in-situ polymerization, where the nanofibers were immersed in a Pyrrole monomer solution which were oxidized to Polypyrrole in the presence of $FeCl_3$. The as treated fibers were carbonized and a Nitrogen content of 12.53at% was reported. The Polypyrrole functionalized CNF was used as an electrode in Li-ion battery and found to have better ORR catalytic activity.

Gan *et al* also utilized Polypyrrole as a nitrogen dopant for CNF in capacitors [29]. In this work, CNFs obtained after electrospinning and carbonization were coated with Graphene and

Polypyrrole by electrodeposition. A three electrode set up was used, with CNF immersed in Graphene Oxide and Pyrrole monomer as the working electrode and a Platinum wire as a counter electrode. Graphene Oxide was reduced to Graphene and was embedded into the Polypyrrole matrix through $\pi - \pi$ stacking and Van-der Waals forces. The graphene/Polypyrrole coated CNF resulted in increased conductivity and improved rate performance.

Wu *et al* reported a facile method of functionalizing carbon nanofibers for improving ORR catalytic activity in fuel cells [30]. They electrospun interconnected Fe-N/C nanofiber networks using Polyvinylpyrollidone and Iron acetylacetonate as precursors . The Nitrogen doping created Pyridine, Pyrolle, Graphitic and Pyridinic Oxide groups in the interconnected fibers. Electron transport between the fibers was enhanced resulting in improved conductivity.

Ye et al combined two concepts of embedding Sulfur nanoparticles in Carbon micropores and utilizing PAN/S composites to improve Lithium-Sulfur performance [31]. A C/S composite was prepared by the conventional thermal treatment method and was mixed with a PAN precursor solution before electrospinning. The resulting fibers were heat treated in an autoclave to cyclize the PAN followed by its sulfurization. The sulfurized PAN nanofibers improved cycle life of Lithium Sulfur battery.

Gu et al reported a two step process to functionalize Graphene with N and P and utilize it as an interlayer [32]. Phosphorus was incorporated into the Graphene matrix by thermal annealing using Triphenylphosphine as a precursor. Nitrogen doping was done by employing a hydrothermal reaction with ammonia solution as the precursor. The resulting composition of N,P in graphene was found to be 4.48% and 1.93% respectively. The functionalized graphene was coated onto a separator and utilized as a polysulfide blocking layer. The addition of N,P also improved the conductivity of graphene.

Motivation of This Work

In this thesis, we attempt to combine the effects of mesoporous carbon and Nitrogen doping on suppressing polysulfide dissolution to improve Lithium Sulfur performance. Air controlled electrospraying and electrospinning techniques were employed in preparation of cell components as well as functionalization.

Chapter 2 of this thesis discusses Cyclization of PAN nanofibers as the method employed for Nitrogen doping. The effects of these Nitrogen doped PAN nanofibers on battery performance was analyzed by testing them as cathodes and interlayers. The system used comprised of a Lithium Anode, Mesoporous CNF(mpCNF) or Mesoporous Cyclized PAN(mpCPAN) as cathode/interlayer and a separator. Eight different combinations of systems were tested:

- mpCNF cathode + mpCNF interlayer
- mpCNF cathode + CPAN interlayer
- CPAN cathode + mpCNF interlayer
- CPAN cathode + CPAN interlayer
- mpCNF cathode + mpCNF interlayer
- mpCNF cathode + mpCPAN interlayer
- mpCPAN cathode + mpCNF interlayer
- mpCPAN cathode + mpCPAN interlayer

It was found that utilizing CPAN as a cell component improved the cycling stability of the cell, particularly when used as an Interlayer. However, contrary to our assumption, the system with CPAN as both cathode and interlayer performed worse than the system with no cell component functionalized, due to significant reduction in mesopores after cyclization. mention activation results. To counter this problem, CPAN fibers were subjected to heat treatment under CO_2, a step that reduced but did not completely eliminate Nitrogen content, and

increased mesopores. In this case, a remarkable improvement in cell performance was observed for the system with both cathode and interlayer functionalized, over the others.

In Chapter 3, we try to address the issue of reduced surface area after Nitrogen doping by employing another technique of Nitrogen Doping. The same system of cell assembly was used as in Chapter 2. In this work, Urea was added to the PAN precursor for electrospinning. The resulting fibers (mpNCNF) were found to have a higher Nitrogen content than mpCNF. Despite the lower Nitrogen content compared to mpCPAN, they had higher content of mesopores.

Four different combinations of systems were tested:

- mpCNF cathode + mpCNF interlayer
- mpCNF cathode + NCNF interlayer
- mpNCNF cathode + mpCNF interlayer
- mpNCNF cathode + NCNF interlayer

It was found that utilizing NCNF as a cell component improved the cycling stability of the cell when used as an Interlayer. mpNCNF had a lower Nitrogen but higher mesopore content and was utilized as cathode/Sulfur host. In this case mpNCNF-NCNF system had the best cycle performance. This was attributed to a synergy between having both high Nitrogen as well as mesopore content in the cell.

In Chapter 4, we briefly discuss the future scope of this work and how we can counter certain limitations in our system to improve cell performance and volumetric energy density, which can further help to provide future insights into commercialization of Lithium-Sulfur batteries.

REFERENCES

[1] D. Bresser, S. Passerini, B. Scrosati, Recent progress and remaining challenges in sulfur-based lithium secondary batteries – a review, Chem. Commun. 49 (2013) 10545. doi:10.1039/c3cc46131a.

[2] N.A. Cañas, K. Hirose, B. Pascucci, N. Wagner, K.A. Friedrich, R. Hiesgen, Investigations of lithium-sulfur batteries using electrochemical impedance spectroscopy, Electrochim. Acta. 97 (2013) 42–51. doi:10.1016/j.electacta.2013.02.101.

[3] A. Manthiram, S.-H. Chung, C. Zu, Lithium-Sulfur Batteries: Progress and Prospects, Adv. Mater. 27 (2015) 1980–2006. doi:10.1002/adma.201405115.

[4] Z.W. Seh, Y. Sun, Q. Zhang, Y. Cui, Designing high-energy lithium–sulfur batteries, Chem. Soc. Rev. 45 (2016) 5605–5634. doi:10.1039/C5CS00410A.

[5] Y.X. Yin, S. Xin, Y.G. Guo, L.J. Wan, Lithium-sulfur batteries: Electrochemistry, materials, and prospects, Angew. Chemie - Int. Ed. 52 (2013) 13186–13200. doi:10.1002/anie.201304762.

[6] A. Manthiram, Y. Fu, S. Chung, C. Zu, Y. Su, Rechargeable Lithium − Sulfur Batteries, (2014). doi:10.1021/cr500062v.

[7] A. Manthiram, S.-H. Chung, C. Zu, Lithium-Sulfur Batteries: Progress and Prospects, Adv. Mater. 27 (2015) 1980–2006. doi:10.1002/adma.201405115.

[8] B.P. Williams, Y.L. Joo, Tunable Large Mesopores in Carbon Nanofiber Interlayers for High-Rate Lithium Sulfur Batteries, J. Electrochem. Soc. 163 (2016) A2745–A2756. doi:10.1149/2.0931613jes.

[9] R. Elazari, G. Salitra, A. Garsuch, A. Panchenko, D. Aurbach, Sulfur-impregnated activated carbon fiber cloth as a binder-free cathode for rechargeable Li-S batteries, Adv. Mater. 23 (2011) 5641–5644. doi:10.1002/adma.201103274.

[10] N. Jayaprakash, J. Shen, S.S. Moganty, A. Corona, L.A. Archer, Porous hollow carbon@sulfur composites for high-power lithium-sulfur batteries, Angew. Chemie - Int. Ed. 50 (2011) 5904–5908. doi:10.1002/anie.201100637.

[11] L. Ji, M. Rao, H. Zheng, L. Zhang, Y. Li, W. Duan, J. Guo, E.J. Cairns, Y. Zhang, Graphene oxide as a sulfur immobilizer in high performance lithium/sulfur cells, J. Am. Chem. Soc. 133 (2011) 18522–18525. doi:10.1021/ja206955k.

[12] J. Schuster, G. He, B. Mandlmeier, T. Yim, K.T. Lee, T. Bein, L.F. Nazar, Spherical ordered mesoporous carbon nanoparticles with high porosity for lithium-sulfur batteries, Angew. Chemie - Int. Ed. 51 (2012) 3591–3595. doi:10.1002/anie.201107817.

[13]H. Wang, Y. Yang, Y. Liang, J.T. Robinson, Y. Li, A. Jackson, Y. Cui, H. Dai, Graphene-wrapped sulfur particles as a rechargeable lithium-sulfur battery cathode material with high capacity and cycling stability, Nano Lett. 11 (2011) 2644–2647. doi:10.1021/nl200658a.

[14] G. Zheng, Y. Yang, J.J. Cha, S.S. Hong, Y. Cui, Hollow carbon nanofiber-encapsulated sulfur cathodes for high specific capacity rechargeable lithium batteries, Nano Lett. 11 (2011) 4462–4467. doi:10.1021/nl2027684.

[15] Y.-S.S. Arumugam Manthiram, Lithium-Sulfur Batteries with Porous Carbon Interlayer Configurations, 5904 (2012) 8817. doi:10.1038/ncomms2163.

[16] T.Z. Hou, H.J. Peng, J.Q. Huang, Q. Zhang, B. Li, The formation of strong-couple interactions between nitrogen-doped graphene and sulfur/lithium (poly)sulfides in lithium-sulfur batteries, 2D Mater. 2 (2015). doi:10.1088/2053-1583/2/1/014011.

[17] F. Li, Y. Su, J. Zhao, Shuttle inhibition by chemical adsorption of lithium polysulfides in B and N co-doped graphene for Li–S batteries, Phys. Chem. Chem. Phys. 18 (2016) 25241–25248. doi:10.1039/C6CP04071C.

[18] L. Ma, H.L. Zhuang, S. Wei, K.E. Hendrickson, M.S. Kim, G. Cohn, R.G. Hennig, L.A. Archer, Enhanced Li-S batteries using amine-functionalized carbon nanotubes in the cathode, ACS Nano. 10 (2016) 1050–1059. doi:10.1021/acsnano.5b06373.

[19] Q. Pang, J. Tang, H. Huang, X. Liang, C. Hart, K.C. Tam, L.F. Nazar, A Nitrogen and Sulfur Dual-Doped Carbon Derived from Polyrhodanine@Cellulose for Advanced Lithium-Sulfur Batteries, Adv. Mater. 27 (2015) 6021–6028. doi:10.1002/adma.201502467.

[20] Z.W. Seh, H. Wang, P.-C. Hsu, Q. Zhang, W. Li, G. Zheng, H. Yao, Y. Cui, Facile synthesis of Li_2S–polypyrrole composite structures for high-performance Li2S cathodes, Energy Environ. Sci. 7 (2014) 672. doi:10.1039/c3ee43395a.

[21] L. Wang, Z. Yang, H. Nie, C. Gu, W. Hua, X. Xu, X. Chen, Y. Chen, S. Huang, A lightweight multifunctional interlayer of sulfur–nitrogen dual-doped graphene for ultrafast, long-life lithium–sulfur batteries, J. Mater. Chem. A. 4 (2016) 15343–15352. doi:10.1039/C6TA07027B.

[22] Q. Zeng, X. Leng, K.H. Wu, I.R. Gentle, D.W. Wang, Electroactive cellulose-supported graphene oxide interlayers for Li-S batteries, Carbon N. Y. 93 (2015) 611–619. doi:10.1016/j.carbon.2015.05.095.

[23] G. Zhou, E. Paek, G.S. Hwang, A. Manthiram, Long-life Li/polysulphide batteries with high sulphur loading enabled by lightweight three-dimensional nitrogen/sulphur-codoped graphene sponge, Nat. Commun. 6 (2015) 1–11. doi:10.1038/ncomms8760.

[24] S. Wang, C. Dai, J. Li, L. Zhao, Z. Ren, Y. Ren, Y. Qiu, J. Yu, The effect of different nitrogen sources on the electrocatalytic properties of nitrogen-doped electrospun carbon nanofibers for the oxygen reduction reaction, Int. J. Hydrogen Energy. 40 (2015) 4673–4682. doi:10.1016/j.ijhydene.2015.02.031.

[25] Y. Xu, C. Zhang, M. Zhou, Q. Fu, C. Zhao, M. Wu, Y. Lei, Highly nitrogen-doped carbon nanofibers as potassium-ion battery anodes with superior rate capability and cyclability, Nat. Commun. (n.d.) 1–29. doi:10.1038/s41467-018-04190-z.

[26] C. Chen, Y. Lu, Y. Ge, J. Zhu, H. Jiang, Y. Li, Y. Hu, X. Zhang, Synthesis of Nitrogen-Doped Electrospun Carbon Nanofibers as Anode Material for High-Performance Sodium-Ion Batteries, Energy Technol. 4 (2016) 1440–1449. doi:10.1002/ente.201600205.

[27]L. Chen, X. Cui, Y. Wang, M. Wang, F. Cui, C. Wei, W. Huang, Z. Hua, L. Zhang, J. Shi, One-step hydrothermal synthesis of nitrogen-doped carbon nanotubes as an efficient electrocatalyst for oxygen reduction reactions, Chem. - An Asian J. 9 (2014) 2915–2920. doi:10.1002/asia.201402334.

[28] J. Guo, J. Liu, H. Dai, R. Zhou, T. Wang, C. Zhang, S. Ding, H. guo Wang, Nitrogen doped carbon nanofiber derived from polypyrrole functionalized polyacrylonitrile for applications in lithium-ion batteries and oxygen reduction reaction, J. Colloid Interface Sci. 507 (2017) 154–161. doi:10.1016/j.jcis.2017.07.117.

[29] J.K. Gan, Y.S. Lim, A. Pandikumar, N.M. Huang, H.N. Lim, Graphene/polypyrrole-coated carbon nanofiber core–shell architecture electrode for electrochemical capacitors, RSC Adv. 5 (2015) 12692–12699. doi:10.1039/C4RA14922J.

[30] N. Wu, Y. Wang, Y. Lei, B. Wang, C. Han, Y. Gou, Q. Shi, Electrospun interconnected Fe-N / C nanofiber networks as efficient electrocatalysts for oxygen reduction reaction in acidic media, Nat. Publ. Gr. (2015) 1–9. doi:10.1038/srep17396.

[31]J. Ye, F. He, J. Nie, Y. Cao, H. Yang, X. Ai, capacity cathode for lithium – sulfur batteries †, J. Mater. Chem. A Mater. Energy Sustain. 3 (2015) 7406–7412. doi:10.1039/C4TA06976E.

[32]L.L. Beijing, C. Science, Porous nitrogen and phosphorous dual doped graphene blocking layer for high performance Li–S batteries, (2016). doi:10.1039/C5TA04255K.

CHAPTER 2

COMBINING THE EFFECTS OF MESOPOROUS CARBON AND NITROGEN GROUPS TO ENHANCE POLYSULFIDE ENTRAPMENT IN LITHIUM-SULFUR BATTERIES

Keywords: Lithium Sulfur Batteries, Mesoporous carbon nanofiber, gas assisted electrospinning, air-controlled electrospray

Highlights:

- Gas assisted electrospinning of Polyacrylionitrile solutions was used to make mesoporous carbon nanofibers for electrodes and interlayers.
- Mesoporous carbon nanofibers were functionalized with cyclic Nitrogen groups.
- Performance of Nitrogen functionalized nanofibers as cathode and interlayer was compared.

ABSTRACT

Rechargeable Lithium Sulfur batteries have attracted widespread attention due to their high theoretical energy density, which is of great importance due to growing energy demands. These batteries have not been commercialized due to the challenges caused by their complex electrochemical reactions such as the shuttle effect and solubility of higher order Polysulfides in the electrolytes. In this paper, we attempt to combine different physical and chemical modifications through the incorporation of mesoporous carbon electrodes, interlayers and Nitrogen groups using Gas-Assisted electrospinning and electrospraying techniques. We also compare the synergistic effects off all these features on battery performance and use various characterization tools to understand them

1. INTRODUCTION

As demand for energy increases, there is a growing need for clean, efficient and cost effective renewable energy sources and reduce the usage of fossil fuels. Lithium Sulfur batteries have a high theoretical energy density of 2600 Wh/kg and a specific capacity of 1675 mAh/g. Sulfur is abundantly available and is environmentally benign [1-3]. All these reasons make Lithium Sulfur batteries among one of the most promising next generation rechargeable batteries. However, Lithium Sulfur batteries face several challenges in performance that need to be resolved before they can be commercially viable. One of these is the dissolution of higher order polysulfides into the electrolyte, which makes it difficult to recover them as Lithium Sulfide precipitate on the cathode at the end of discharge cycle, leading to loss of active material and low capacity. Another challenge is the polysulfide shuttle effect, when the higher order polysulfides migrate to the anode, get reduced to Li_2S and migrate back to the cathode to get reoxidized. The insulating nature of Sulfur and Lithium Sulfide also adds to the cell resistance [4-7].

Several efforts have been made to combat the technical issues mentioned above. It has been found that several types of carbon nanomaterials such as microporous carbon, mesoporous carbon, hierarchical porous carbon, carbon black, hollow carbon spheres, CNTs, CNFs, reduced graphene oxide and graphene can improve cell performance. These porous carbons can contain the active material, constrain the dissolved polysulfides, and accelerate charge/electron transport [8-14]. Manthiram et al introduced the concept of inserting an interlayer between the cathode and separator to acts as a polysulfide entrapper and enhance the reutilization of trapped material. However, despite the improved performance, this acts as a temporary solution since the interlayer acts as only a physical barrier and the polysulfides can eventually leach out to the electrolyte [15].

To ensure more permanent constraining of polysulfides, chemical modification of active hosts surface are also effective in reducing shuttle effect and improving cycle performance. Introduction of doping elements like Nitrogen, Sulfur, Phosphorus, Boron have been shown formation of strong chemical bonds between the polysulfides and these elements[16,17]. Nitrogen doping has been done by introducing electron-rich functional groups like Amines, polypyrrole, pyrroles, pyridines and has been found to be effective in assisting mesoporous carbon in suppressing polysulfide shuttling effect through Lewis Acid-Base interactions with polysulfides[18-23].

In this paper, we study and compare the results of functionalizing mesoporous Carbon cathodes and interlayers with electron rich Nitrogen groups. Mesoporous Carbon nanofiber webs were synthesized by gas assisted electrospinning of Polyacrylonitrile solutions , and used as both cathode and interlayer in our system. Cathodes were prepared by electrospraying Sulfur onto Mesoporous Carbon, a facile technique which can be used to created higher loading Sulfur electrodes . The surface chemistry of these mesoporous fibers was modified by introducing cyclic Nitrogen groups . They were then utilized as cathodes and interlayers to test the effects of adding cyclic Nitrogen groups on cell performance .

2. EXPERIMENTAL METHODS

2.1 Synthesis of Mesoporous Carbon Nanofiber web (mpCNF)

Polyacrylonitrile (PAN) (mw=150,000 from Sigma Aldrich) and Poly(methyl methylacrylate) (PMMA) were dissolved in dimethylformamide (DMF) to a 12 wt% polymer content, by stirring at 65^0C for 12 hours [24]. The nanofibers were prepared by gas assisted electrospinning at 15kV, 30 cms distance from the collector at a 0.075ml/min flow rate. An 18 gauge stainless steel needle was used for electrospinning. The nanofibers were stabilized in air

at 280^{0}C for 2 hours, carbonized in Nitrogen at 900^{0}C for 2 hours and activated in Carbon Dioxide at 900^{0}C for 2 hours.

2.2 Synthesis of cyclized-polyacrylonitrile modified CNF fibers (CPAN)

A 5 wt% PAN-PMMA solution in DMF was prepared. The above prepared CNF nanofibers were immersed in the PAN solution for 1 minute and dried at 80^{0}C for 12 hours. The PAN coated mesoporous fiber was heat treated in Argon at 300^{0}C for 10 hours [25].

2.3 Synthesis of mesoporous cyclized-polyacrylonitrile modified CNF fibers (mpCPAN)

The above prepared CPAN fibers underwent a heat treatment activation process under Carbon Dioxide at 700^{0}C for 1hour to improve the mesopore distribution and BET surface area.

2.4 Synthesis of electrodes

The CPAN,mpCPAN and mpCNF electrodes were synthesized by air controlled electrospraying [26]. Sublimed sulfur(Spectrum Chemical Mfg.Corp) and Ketjen Black EC-600JD(KB)(AzkoNobel) solution were dispersed in CS_2 to obtain a composition of 97% Sulfur and 3% Ketjen Black [22] . The solution was stirred for 3 hours and sonicated for 30 minutes before electrospraying on mpCNF and mpCPAN webs at 15kV, 10 cms distance from the collector at 0.08ml/min flow rate. An 18 gauge stainless steel needle was used for air controlled electrospraying. Electrospraying was carried out until the target Sulfur loading was deposited on the cathode. Cathodes with Sulfur loading of 1.1mg/cm^2 and 1.7mg/cm^2 were used for testing. Sulfur content of the substrates was 14.3% for 1.1mg/cm^2 and 21.4% for 1.7mg/cm^2.

2.5 Material Characterization

The pore size distribution analysis was performed on a Micrometrics Gemini VII 2390t in liquid Nitrogen with the Brunauer, Emmett and Teller (BET) method. Samples were degassed under nitrogen at 300^{0}C for at least 3 hours. The scanning electron microscope (SEM) images were taken by a TESCAN Mira3 Field Emission SEM and Zeiss Gemini 500 SEM . The

Fourier Transform infrared (FTIR) spectra of mpCNF and mpCPAN was carried out using a Bruker-Hyperion FT-IR Microscope at ambient temperature. X-ray Photoelectron spectroscopy (XPS) of mpCPAN and mpCNF before and after cycling was used to obtain chemical bonding information and elemental analysis.

2.6 Electrochemical Characterization

The interlayers and substrates were cut into discs of diameter 15 mm from the nanofiber mat. CR2032 coin cells were assembled using Sulfur deposited mpCPAN/mpCNF (5.5mg/cm^2) as cathodes, Lithium metal (same diameter as cathode) as anode, mpCPAN/mpCNF (8.2mg/cm^2) as interlayers, a 25 micron thick Celgard separator and an electrolyte of 1M lithium bis-(trifluromethanesulfone)imide and 0.2M $LiNO_3$ in 1,2-dioxolane/1,2-dimethoxyethane (v/v=1:1). EIS measurements were carried out using a Solartorn Cell Test System model 1470E potentiostat between frequencies 0.01-100kHz.

3. RESULTS AND DISCUSSION

Various analytical tools were used to characterize the surfaces of CPAN,mpCNF and mpCPAN and confirm the presence of cyclic Nitrogen groups in mpCPAN after synthesis. XPS survey scans of CPAN, mpCNF and mpCPAN are presented in Fig 1 (a). Before the cyclization reaction, for mpCNF, we see 2 prominent peaks for C 1s at 285eV and O 1s at 532eV. For CPAN and mpCPAN, we see a third prominent peak for N 1s at 400eV. However, as seen in Fig1(b), the intensity of the Nitrogen peak is significantly higher for CPAN as opposed to mpCPAN, indicative of a much higher Nitrogen content. Fig 1(c) and(d) shows the deconvoluted N 1s signals for CPAN and mpCPAN respectively, with 2 peaks for pyridine and pyrrole at 398eV and 399.9 eV respectively[23-26]

(a)

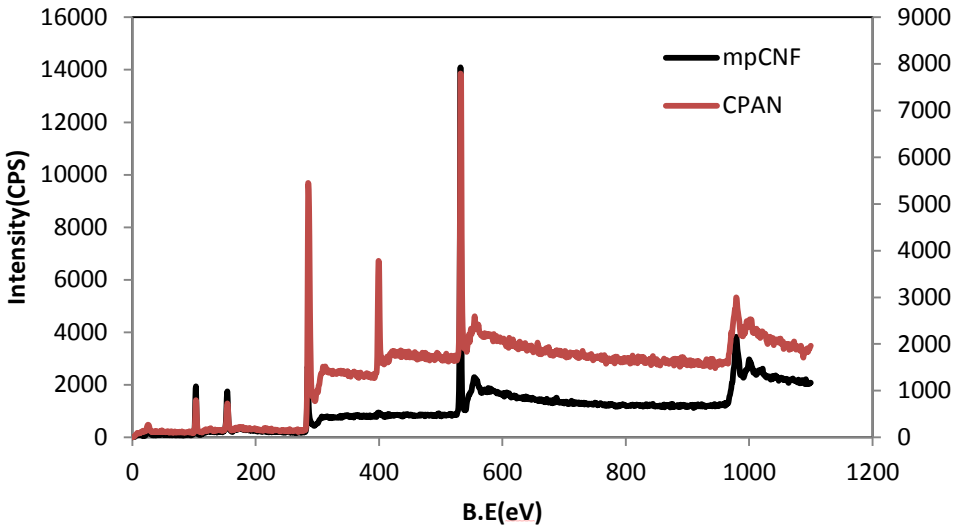
16000
14000
12000
10000
8000
6000
4000
2000
0
9000
8000
7000
6000
5000
4000
3000
2000
1000
0
0
200
400
600
800
1000
1200
Intensity(CPS)
B.E(eV)
mpCNF
CPAN

(b)

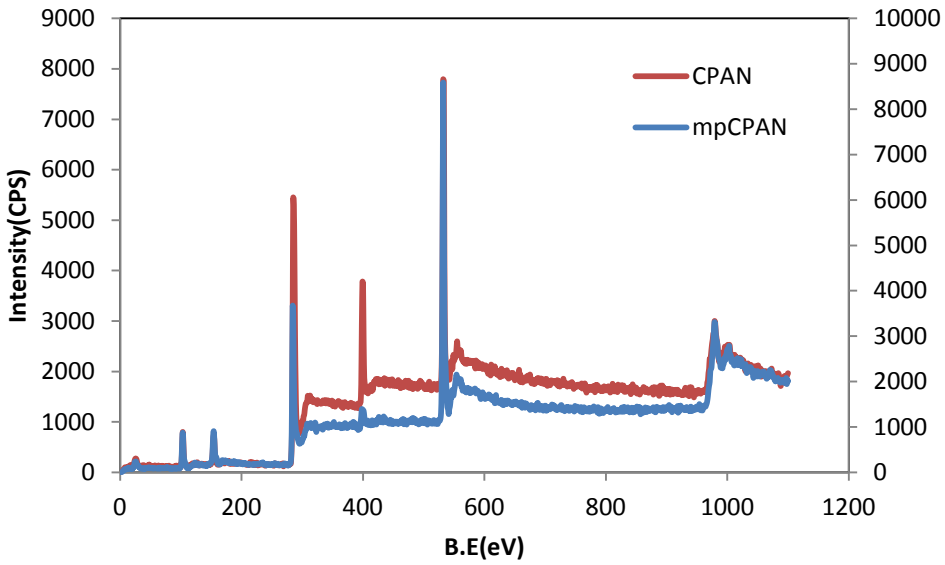
9000
8000
7000
6000
5000
4000
3000
2000
1000
0
10000
9000
8000
7000
6000
5000
4000
3000
2000
1000
0
0
200
400
600
800
1000
1200
Intensity(CPS)
B.E(eV)
CPAN
mpCPAN

(c)

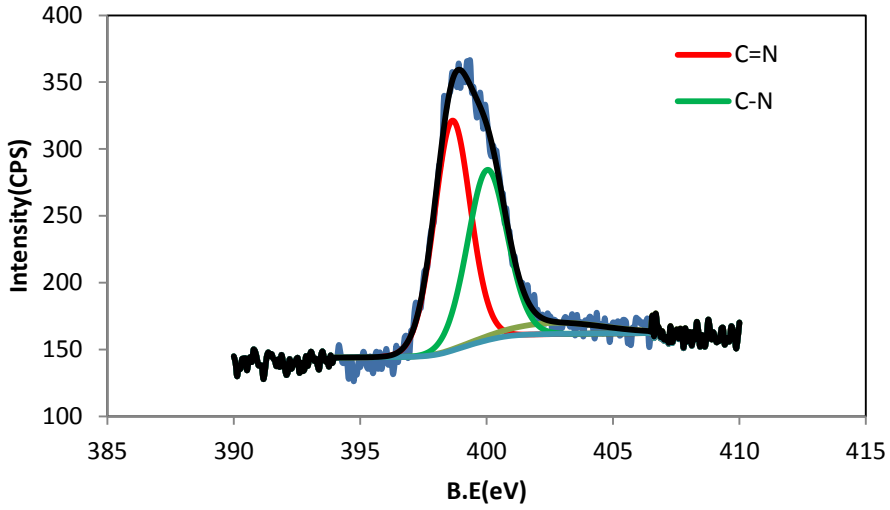

(d)

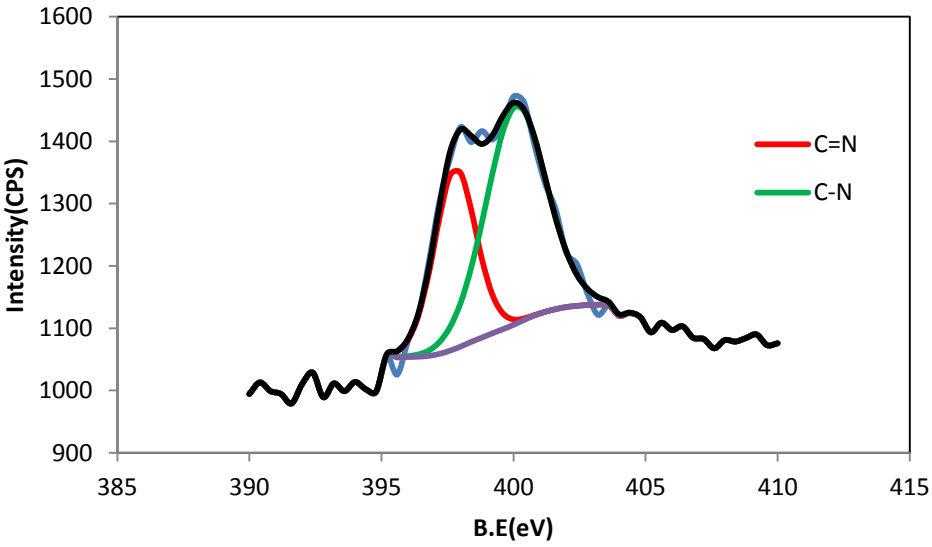

Fig 1. (a) XPS survey scanning spectra for mpCNF and and CPAN (b) XPS survey scanning spectra for mpCPAN and and CPAN (c) High Resolution N 1s spectra of CPAN (d)) High Resolution N 1s spectra of mpCPAN

FTIR spectra of CPAN in Fig 2 shows absorbance bands at approximately 1066,1150 and 1195 cm^{-1} which represent C-N stretching. The peak at 1560cm^{-1} represents the vibration of combined C=C and C=N and the peak around 1370cm^{-1} is for C-C stretching [23-26].

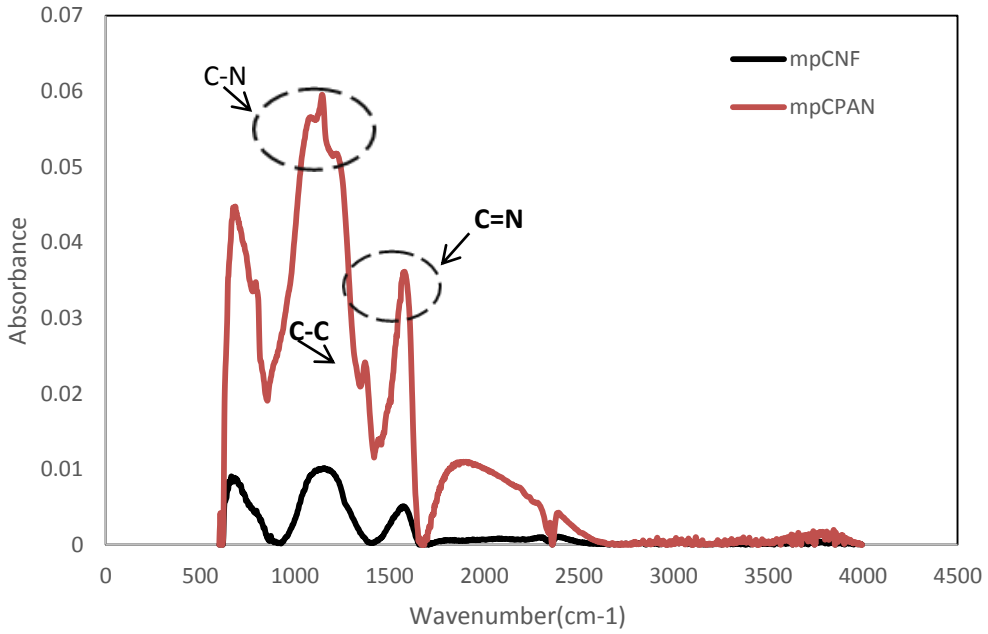

Fig 2. Experimental FTIR spectra of mpCNF and mpCPAN

The structure and morphology of mpCPAN and mpCNF were analyzed to deduce the reasons behind the findings obtained from XPS. SEM images of mpCNF and mpCPAN are shown in Fig 3 (a),(b). We find that mpCNF has a larger number of pores compared to CPAN. It appears that the dip-coating treatment used to synthesize mpCPAN, resulted in the nanofibers adhering together.

(a)

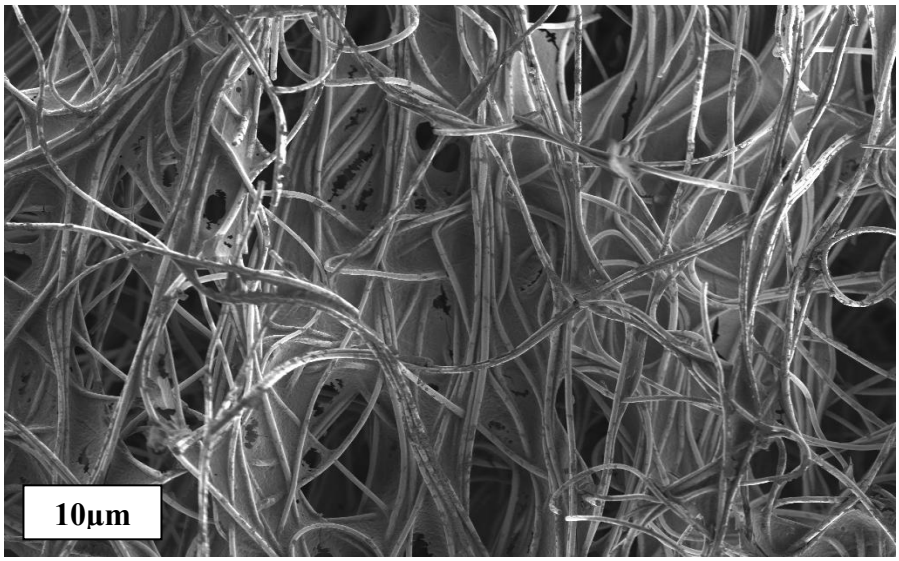

(b)

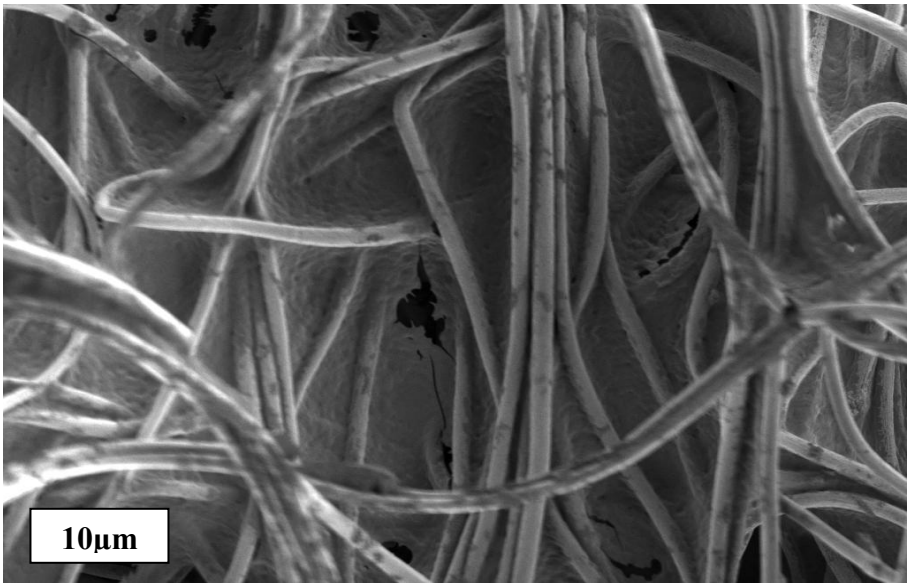

(c)

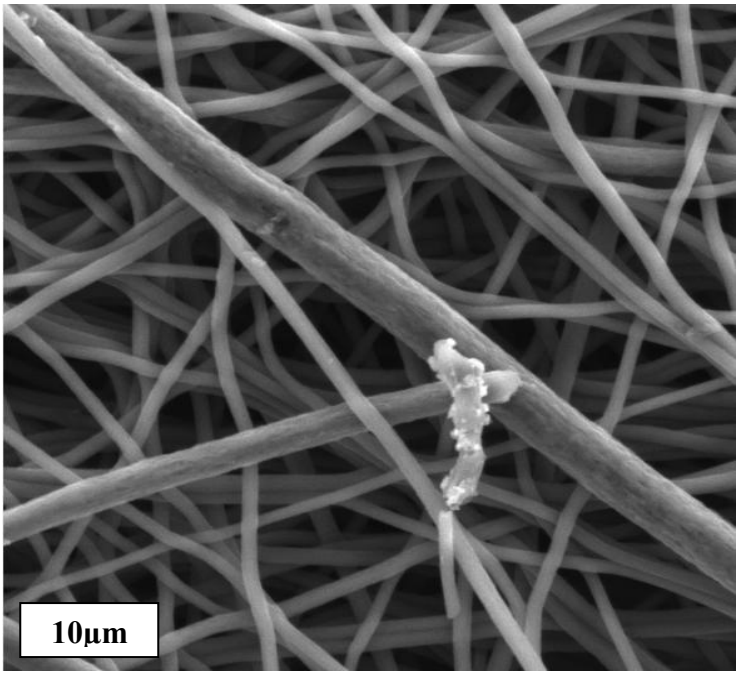

Fig 3. SEM images of (a) CPAN (b) CPAN and (c) mpCNF

The BET surface area reduced significantly from 504.28 m²/g to 32 m²/g during the synthesis.

The pore size distribution of mpCNF and CPAN are shown in Fig 4.

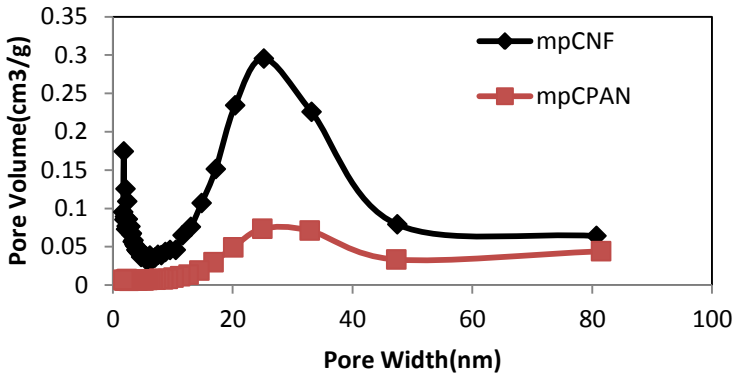

Fig 4. Comparison of pore size distribution of mpCNF and mpCPAN

However, on activation of CPAN, the BET surface area was increased to 300.6336 m^2/g and a corresponding increase in mesopore volume was also observed as shown in Fig 5.

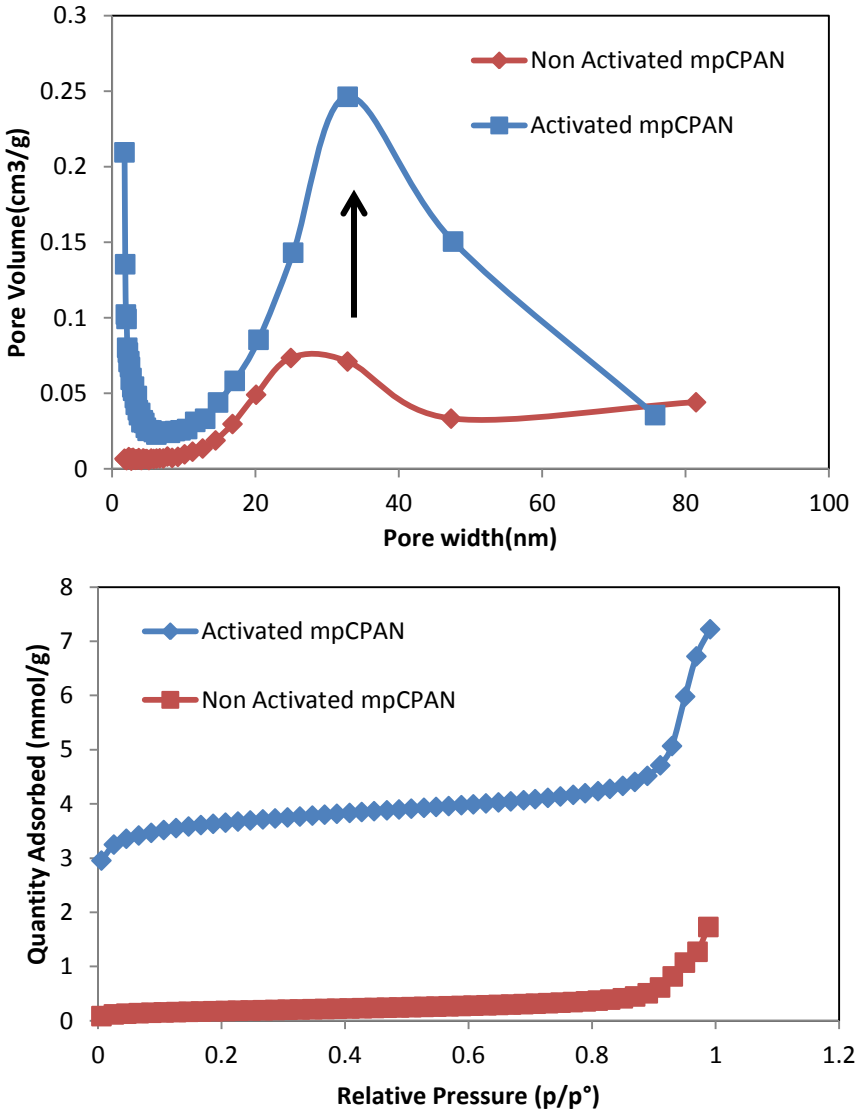

Fig 5. (a) pore size distribution of CPAN and mpCPAN (b) Nitrogen adsorption isotherm for mpCPAN and CPAN

Having confirmed the cyclization of mpCNF, the effects of CPAN,mpCNF and mpCPAN on the electrochemical performance of the cells was tested by using them as both cathodes and interlayers in the following combinations of systems:

- mpCNF cathode and mpCNF interlayer (mpCNF-mpCNF)
- mpCNF cathode and CPAN interlayer (mpCNF-CPAN)
- CPAN cathode and mpCNF interlayer (CPAN-mpCNF)
- CPAN cathode and CPAN interlayer (CPAN-CPAN)
- mpCNF cathode and mpCNF interlayer (mpCNF-mpCNF)
- mpCNF cathode and mpCPAN interlayer (mpCNF-mpCPAN)
- mpCPAN cathode and mpCNF interlayer (mpCPAN-mpCNF)
- mpCPAN cathode and mpCPAN interlayer (mpCPAN-mpCPAN)

Cycle performances were carried out at 0.25C for 100 cycles using sulfur loadings 1.1mg/cm^2 and 1.7mg/cm^2. As seen in Fig 3 and Fig 4, for both the sulfur loadings, we find that system mpCNF-CPAN displays highest capacity and best capacity retention. Interestingly, system CPAN-CPAN has the lowest capacity, performing poorly compared to system mpCNF-mpCNF which has no nitrogen functional groups. Rate capability tests of the above systems were compared at both loadings. Rate capability tests indicate that using CPAN as cathode may not be suitable for higher Sulfur loadings and higher C-rates.

(a)

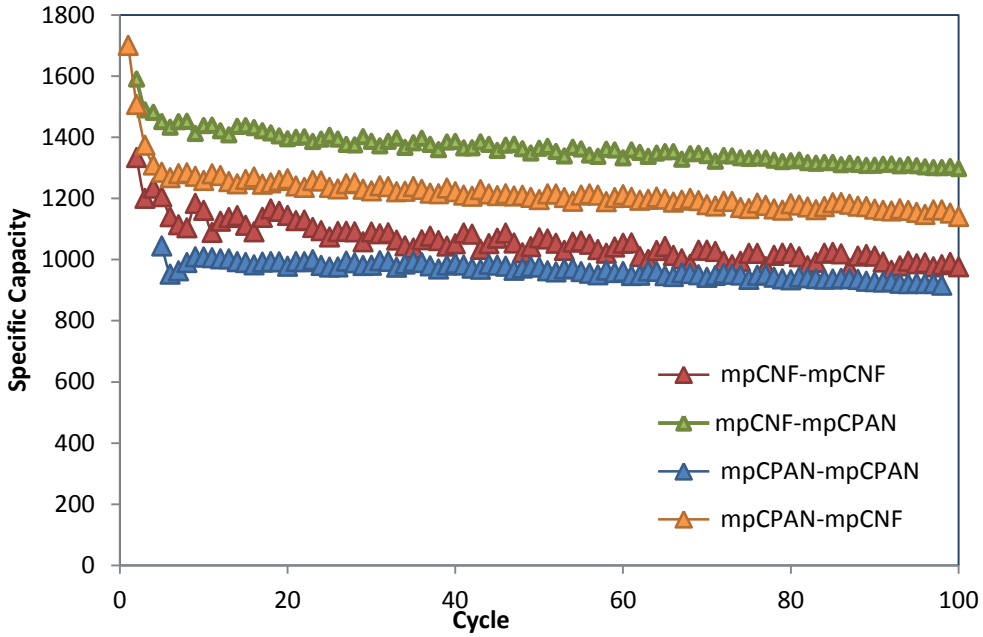
Specific Capacity
Cycle
mpCNF-mpCNF
mpCNF-mpCPAN
mpCPAN-mpCPAN
mpCPAN-mpCNF

(b)

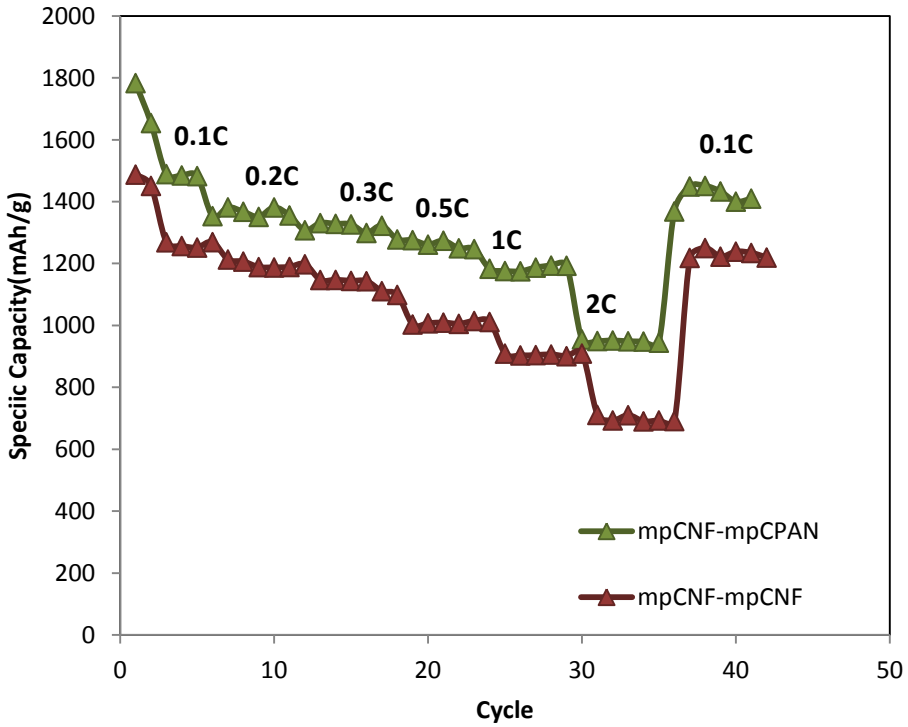
Speciic Capacity(mAh/g)
Cycle
0.1C
0.2C
0.3C
0.5C
1C
2C
0.1C
mpCNF-mpCPAN
mpCNF-mpCNF

(c)

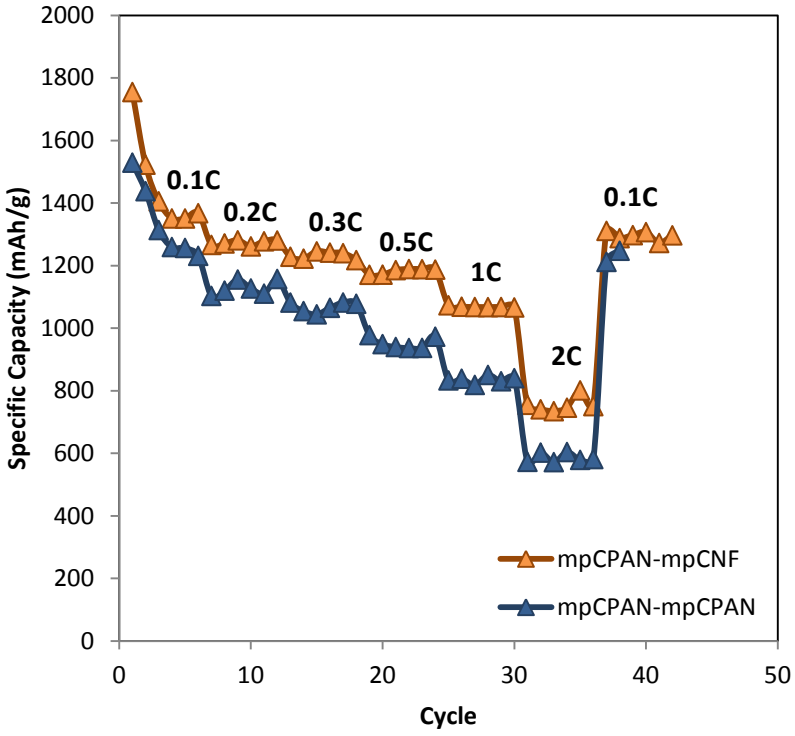

Fig 6. (a) Cycling performance of 4 systems at 1.1mg/cm^2 S-loading, 0.25C (b) Rate Capability test comparison of systems using CPAN as interlayer at 1.1mg/cm^2 S-loading (c) Rate Capability test comparison of systems using CPAN as cathode at 1.1mg/cm^2 S-loading

(a)

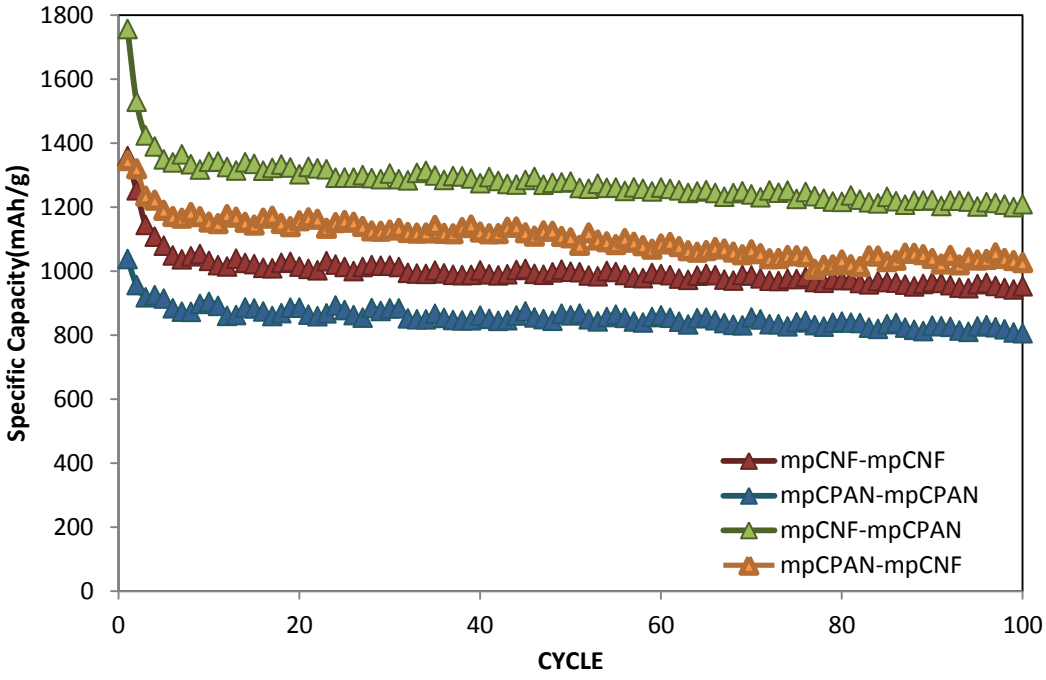
1800
1600
1400
1200
1000
800
600
400
200
0
Specific Capacity(mAh/g)
0
20
40
60
80
100
CYCLE
mpCNF-mpCNF
mpCPAN-mpCPAN
mpCNF-mpCPAN
mpCPAN-mpCNF

(b)

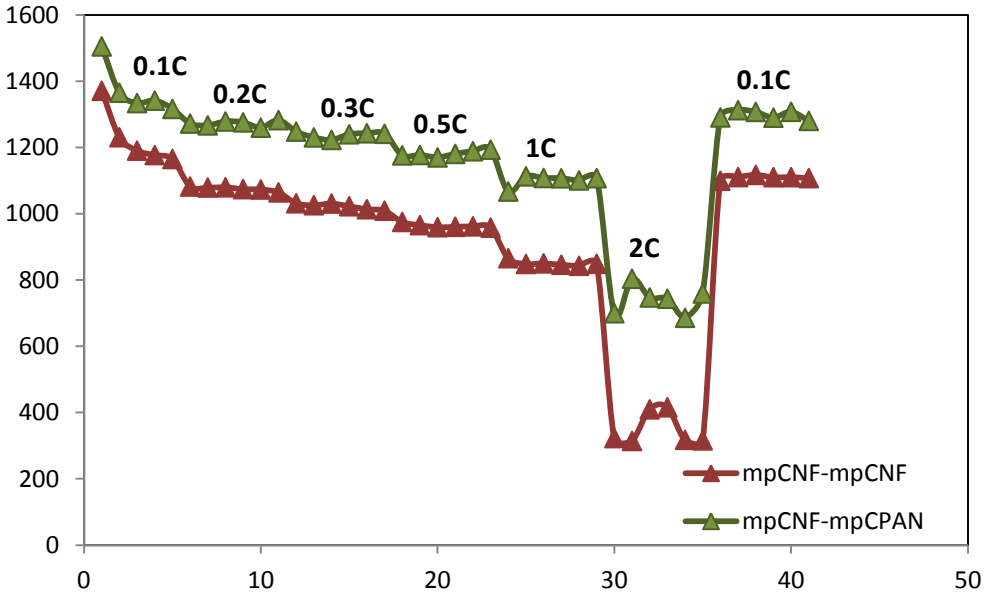
1600
1400
1200
1000
800
600
400
200
0
0.1C
0.2C
0.3C
0.5C
1C
2C
0.1C
0
10
20
30
40
50
mpCNF-mpCNF
mpCNF-mpCPAN

(c)

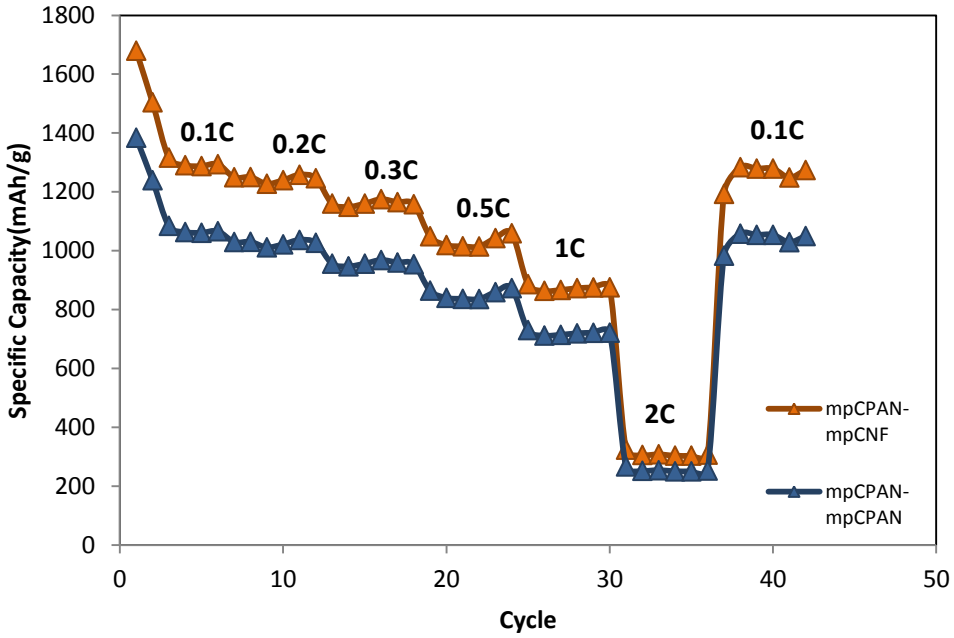

Fig7. (a) Cycling performance of 4 systems at 1.7mg/cm^2 S-loading, 0.25C (b) Rate Capability test comparison of systems using CPAN as interlayer at 1.7mg/cm^2 S-loading (c) Rate Capability test comparison of systems using CPAN as cathode at 1.7mg/cm^2 S-loading

In Fig 8, the cycle performance and rate capability of systems utilizing mpCPAN was examined for S-loading of 1.1 mg/cm^2. In this case, due to the lower Nitrogen content of mpCPAN, mpCNF-mpCPAN system had a lower capacity compared to their non-activated counter part. However, the mpCPAN-mpCPAN system had a cycle performance and rate capability comparable to that of mpCNF-CPAN system. This may be due to the presence of mesopores and nitrogen groups in both the cathode and interlayer, leading to greater polysulfide confinement.

(a)

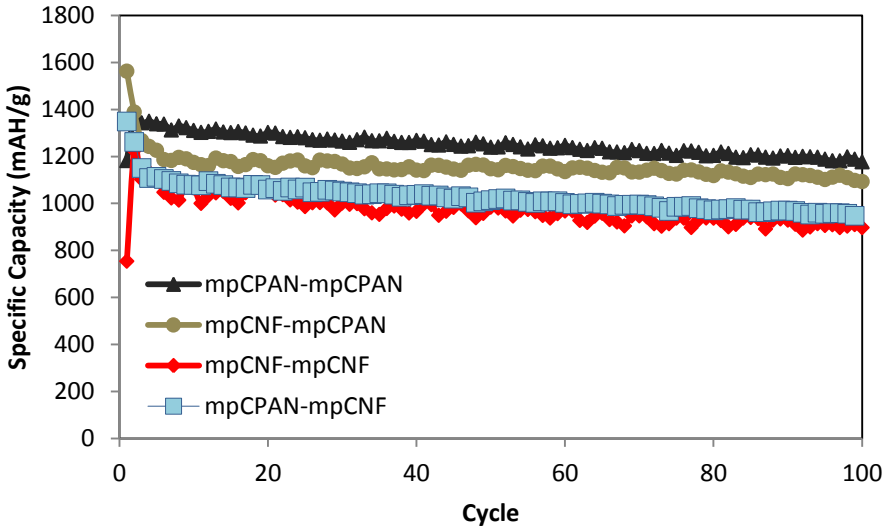

(b)

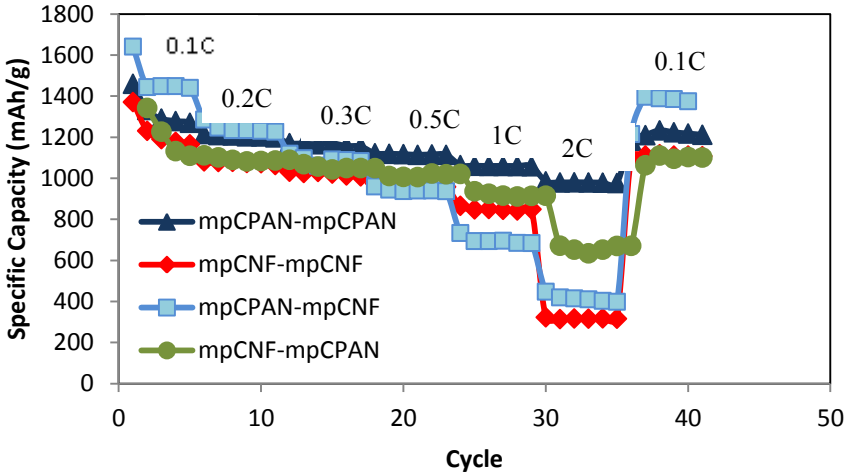

Fig 8. (a) Cycling performance of 4 systems at 1.1mg/cm^2 S-loading, 0.25C (b) Rate Capability test comparison of systems using mpCPAN as interlayer/cathodes at 1.1mg/cm^2 S-loading

Various characterization tools were used to deduce the reasons behind the lower capacity of CPAN-CPAN system compared to mpCPAN-mpCPAN as well as the chemical changes that occur in the different systems after several cycles.

Electrochemical Impedance Spectroscopy (EIS) of fresh cells are shown in Fig 6. The EIS spectra of each system consists of 1 semicircle (Charge transfer resistance, R_{ct}) and slope line (Warburg Resistance). Fresh cells, except the CPAN-CPAN system show comparable R_{ct} values indicating similar conductivity. However, CPAN-CPAN system has higher R_{ct} values compared to the remaining 3 systems. EIS spectra of each system after 100 cycles was also compared, as shown in Fig6(c),(d). To compare the polysulfide reutilization capability of each system, the cells were charged to 2.8V before measuring the EIS spectra. It was observed that systems mpCNF-CPAN and CPAN-mpCNF showed a greater reduction in R_{ct} after 100 cycles. More importantly, they retained one semicircle even after charging as opposed to mpCNF-mpCNF and CPAN-CPAN systems. In the latter 2 systems, a second semicircle emerged in the high frequency region, which is attributed to increased surface impedance due to formation of Li_2S precipitate film on the cathode surface [27,28]. This indicates that during the charge cycle, not all the polysulfides were converted back to Sulfur, implying poor Sulfur reutilization capability of mpCNF-mpCNF and CPAN-CPAN systems

(a)

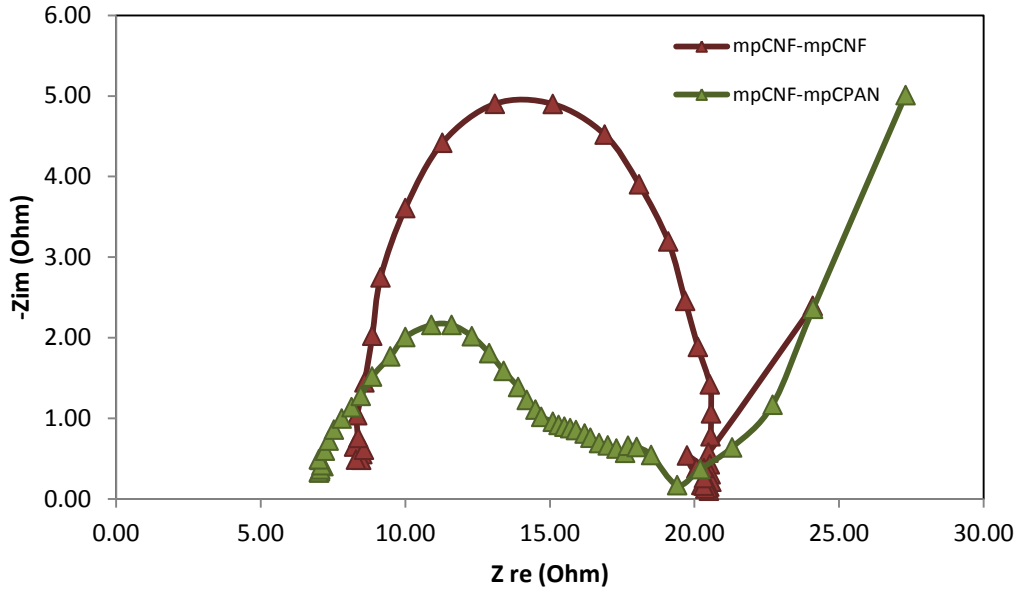
mpCNF-mpCNF
mpCNF-mpCPAN
-Zim (Ohm)
Z re (Ohm)
6.00
5.00
4.00
3.00
2.00
1.00
0.00
0.00
5.00
10.00
15.00
20.00
25.00
30.00

(b)

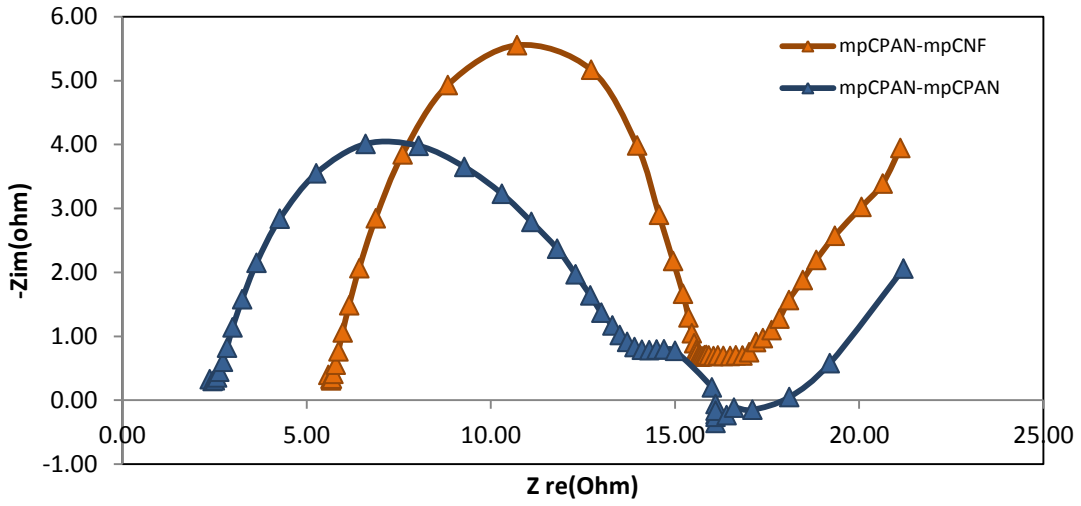
mpCPAN-mpCNF
mpCPAN-mpCPAN
-Zim(ohm)
Z re(Ohm)
6.00
5.00
4.00
3.00
2.00
1.00
0.00
-1.00
0.00
5.00
10.00
15.00
20.00
25.00

(c)

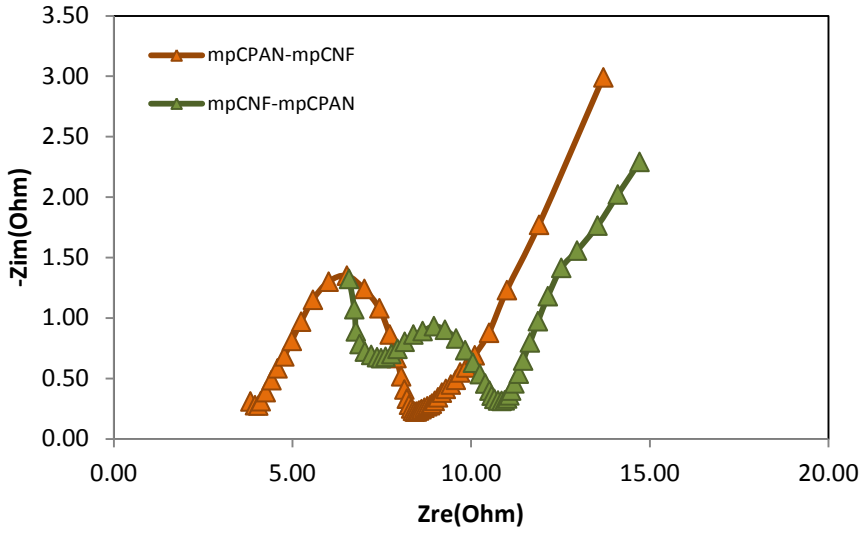

(d)

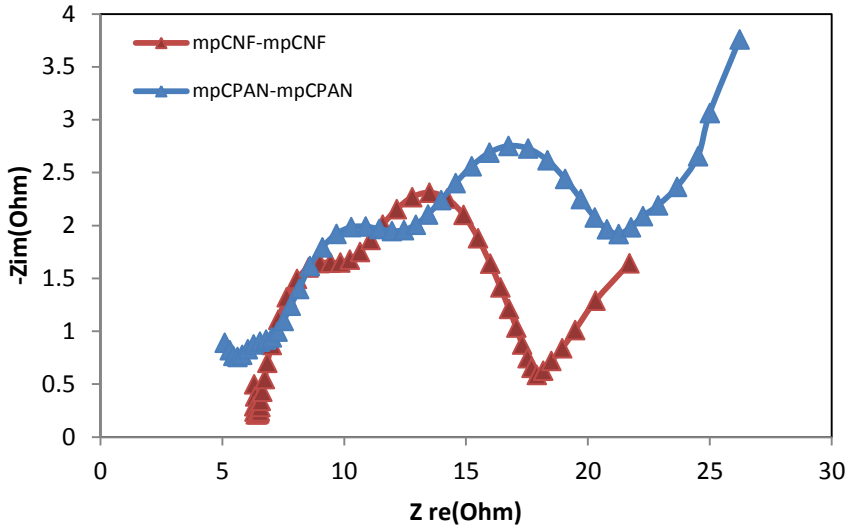

Fig 9. (a) EIS Spectra of fresh cells mpCNF-mpCNF vs mpCNF-CPAN (b) EIS Spectra of fresh cells CPAN-CNF vs CPAN-CPAN (c) EIS Spectra of charged cells mpCNF-CPAN vs CPAN-CNF after 100 cycles (d) EIS Spectra of charged cells mpCNF-mpCNF vs CPAN-CPAN after 100 cycles

In case of mpCPAN systems however, as seen in Fig 10, only the mpCNF-mpCNF and mpCPAN-mpCNF systems had an additional semi-circle after discharging, corresponding to Li_2S precipitate film. Since these systems have mpCNF as interlayer, the polysulfides get deposited between the fibers, but may not be reutilized efficiently in the following charging-discharging cycles . For fresh cells, the charge transfer resistance of cells with at least 1 N-doped component was lower than the reference mpCNF-mpCNF system.

(a)

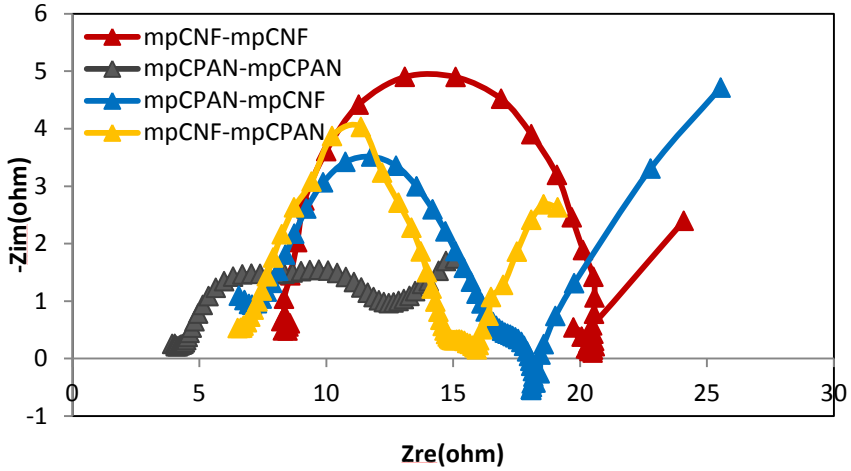

(b)

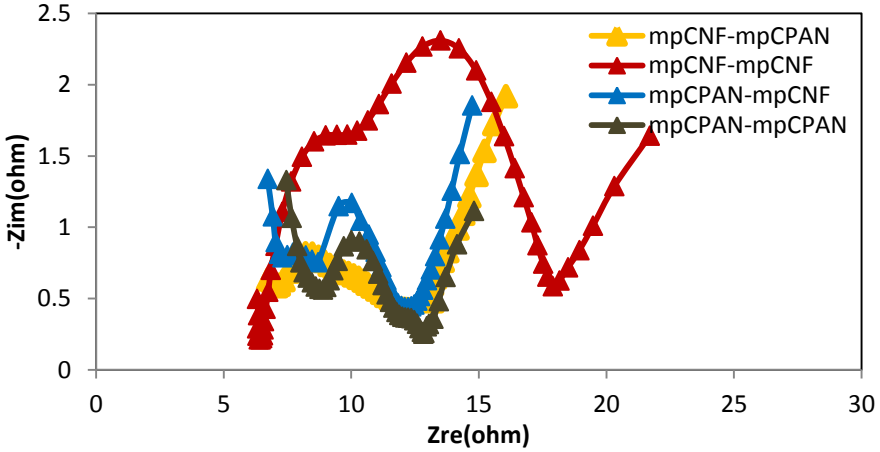

Fig 10.(a)EIS Spectra of fresh cells (b) EIS Spectra of discharged cells after 100 cycles

High resolution S 2p spectra of the cathode and interlayer of each system was examined after 100 cycles and are shown in Fig 11 (a)-(d). The cells were fully discharged to 1.8V. In each system, a sulfate peak at 166.7eV was observed, which can be attributed to reaction of the polysulfides with air/moisture on exposure [29]. An additional signal was observed at 158ev which is attributed to trapped Lithium Polysulfides [29-32]. The higher intensity of the polysulfide peak in CPAN cathodes and interlayers confirms that their polysulfide reutilization capability is better than that of mpCNF. Moreover, The Li_2S signals are significantly weaker in the CPAN cathode as opposed to CPAN interlayer. This implies that despite the presence of Nitrogen functional groups utilizing CPAN as a cathode results in greater active material loss than mpCNF cathode, possibly due to the lack of mesopores.

(a)

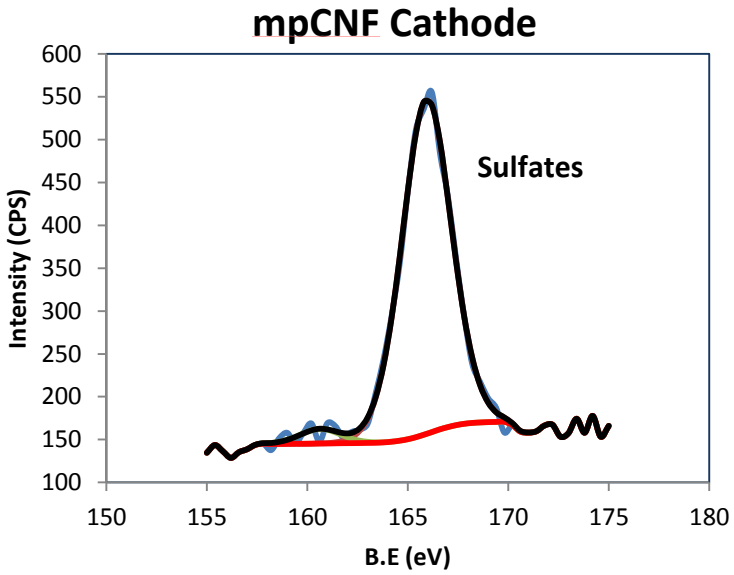

(b)

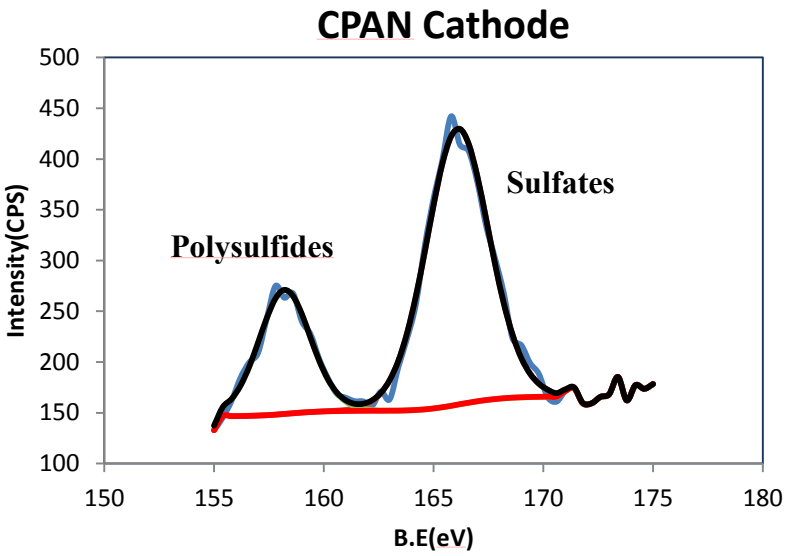
CPAN Cathode
Intensity(CPS)
500
450
400
350
300
250
200
150
100
150
155
160
165
170
175
180
B.E(eV)
Polysulfides
Sulfates

(c)

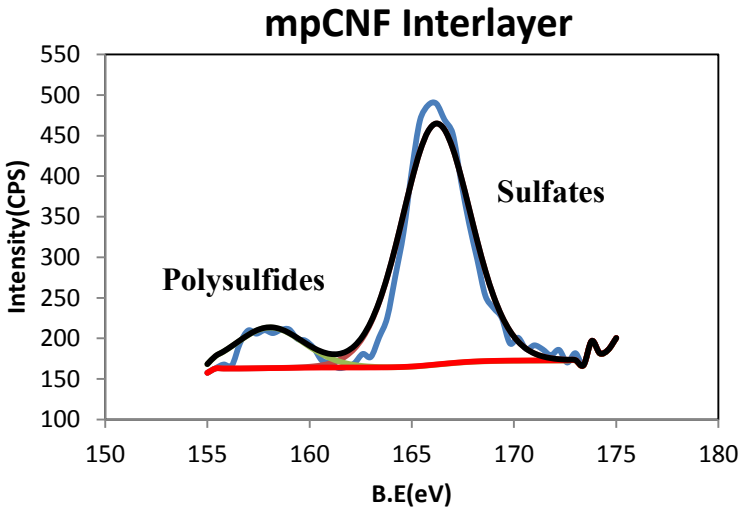
mpCNF Interlayer
Intensity(CPS)
550
500
450
400
350
300
250
200
150
100
150
155
160
165
170
175
180
B.E(eV)
Polysulfides
Sulfates

(d)

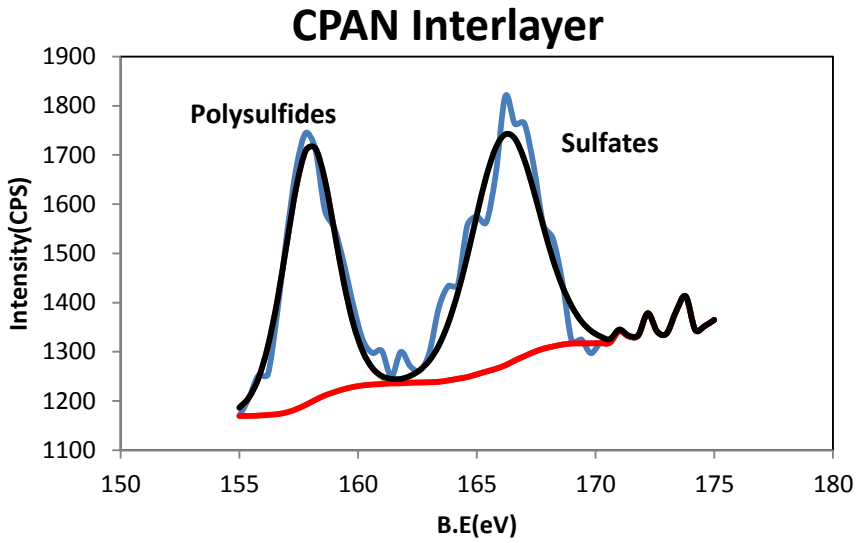

Fig 11. High Resolution S 2p spectra of (a) mpCNF cathode (b) CPAN cathode (c) mpCNF interlayer (d) CPAN interlayer

To further confirm the effectiveness of the Nitrogen groups in capturing Polysulfides, high resolution N 1s spectra of systems utilizing CPAN as cathode or interlayer or both, were examined in Fig 12. The cells were fully discharged to 1.8V. C 1s peaks were calibrated to 284 eV. In the case of mpCNF-CPAN , the N 1s spectra of the interlayer was deconvoluted to obtain 2 peaks at 399.2 and 397eV. Comparing this to the N 1s spectra of pristine CPAN, it appears that the peaks corresponding to Pyrollic and Pyridinc Nitrogen shifted towards a lower binding energy. The peak shifts can be a result of Li-N interaction [33-35]. During Li-N interaction, there is an increased electron density around the more electronegative N atom [35]. The resulting increased shielding effect can reduce the energy required to knock off the electrons. However, it was observed that the shifted peak corresponding to Li-N interactions in CPAN interlayer has a higher intensity and larger area than the peak for cyclic nitrogen groups. This indicates that the interlayer was not the reason behind lower capacity of CPAN-CPAN. Interestingly, for the case of CPAN cathodes, peak deconvolution showed 2 peaks corresponding to Pyridinic Nitrogen and a shifted peak to a binding energy of 395.2 eV. The

peak for Pyridinic Nitrogen had a much larger area and Intensity than the shifted peak, implying that using CPAN as cathode results in poorer Nitrogen group utilization for polysulfide capture. This could explain the poorer cycle performance of CPAN-CPAN relative to the other systems.

(a)

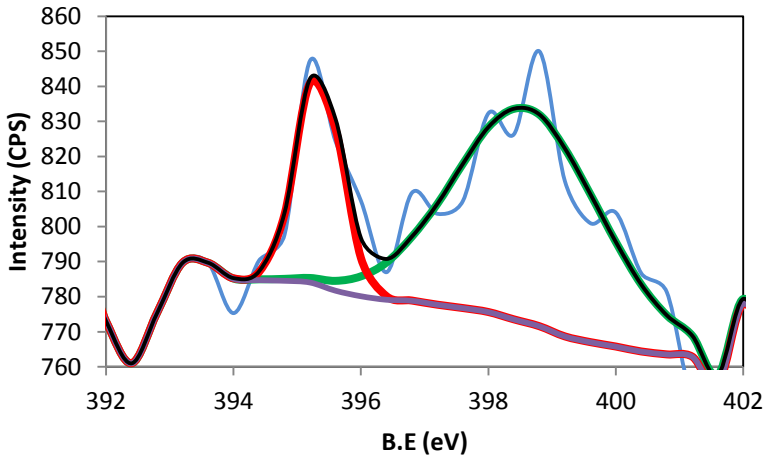

(b)

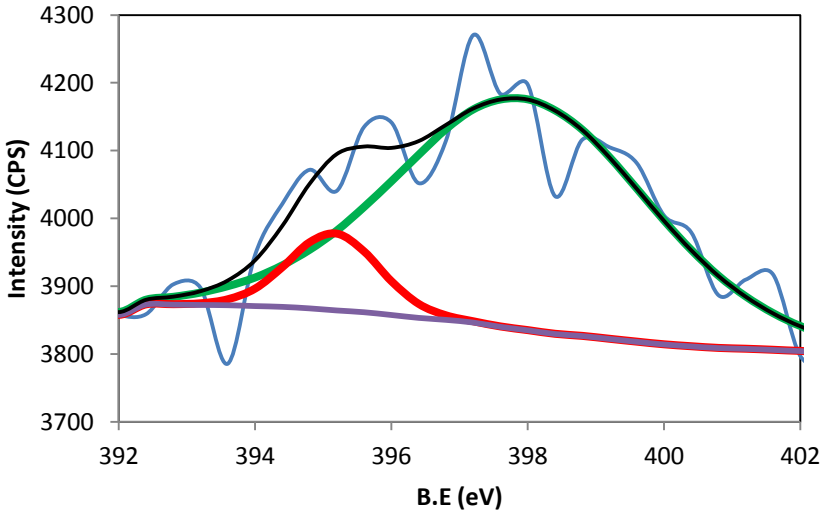

Fig 12. High Resolution N 1s spectra of (a) CPAN interlayer (b) CPAN cathode

High resolution S 2p and N 1s spectra of mpCPAN cathodes and interlayer after discharge cycles are shown in **Fig 13**. An improved utilization of Nitrogen groups in both cathode and interlayer was observed, explaining the improved performance of mpCPAN-mpCPAN system over CPAN-CPAN.

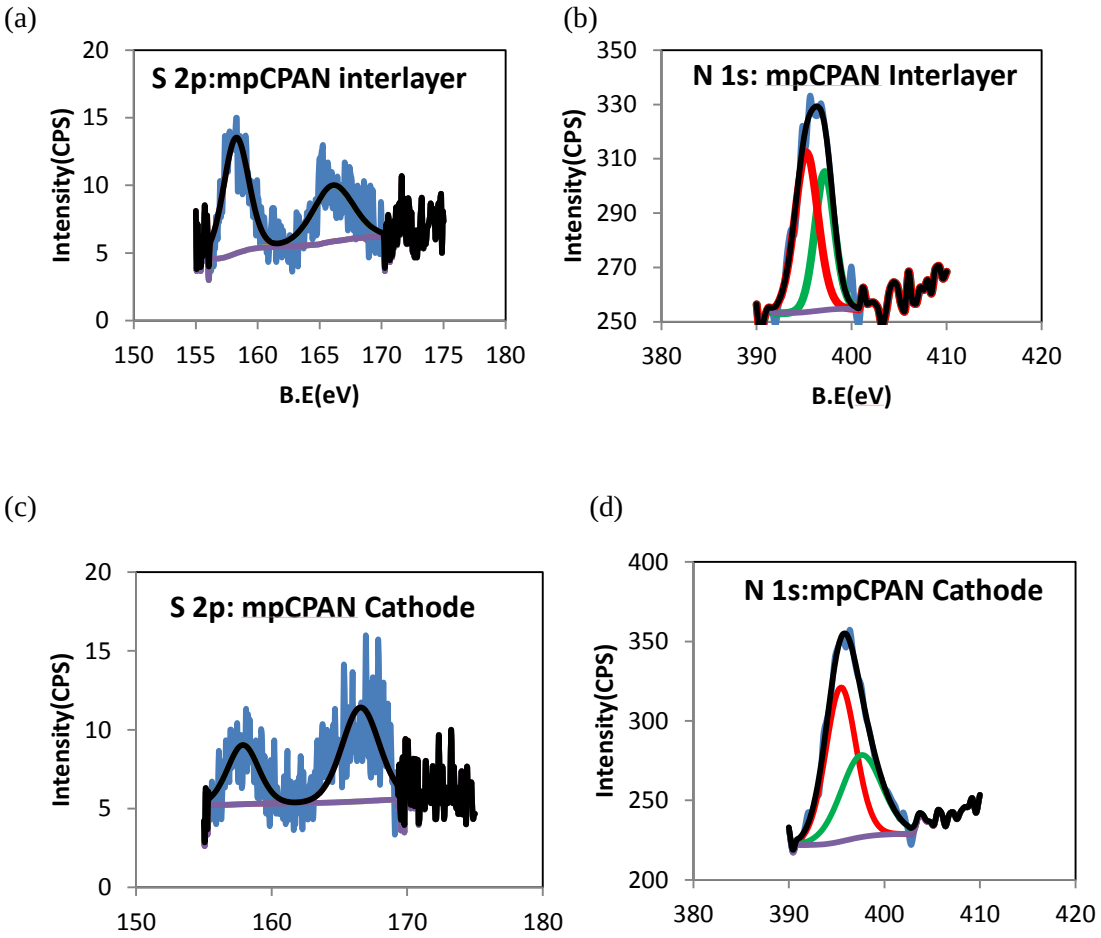

Fig 13. (a)High Resolution S 2p spectra of mpCPAN interlayer (b) High Resolution N 1s spectra of mpCPAN interlayer (c) High Resolution S 2p spectra of mpCPAN cathode (d) High Resolution N 1s spectra of mpCPAN cathode

The significant reduction in surface area and loss of pores in CPAN indicates lower active sites available for Sulfur deposition and electrochemical reactions. This explains why CPAN, with a high N-content but low mesopore volume performs better as an interlayer than a cathode. Sulfur, which was incorporated into the cathode by electrospraying, may have deposited only on the surface of mpCPAN, instead of being trapped in the active pores as it

does in mpCNF. This may have resulted in eventual loss of active material over several cycles. Moreover, the reduced surface area can reduce the Lithium Sulfide storage capability and slow down ion diffusion due to increased tortuosity. In the 4 CPAN systems studied, CPAN-CPAN was the only one that did not have any component with a large surface area and mesopores/micropores. In the remaining 3 systems, there was at least 1 component that had the high surface area required for electrochemical reactions, and therefore they showed a better cycle performance than CPAN-CPAN. However, though mpCNF-mpCNF has both components with a higher surface area, it has a lower capacity and stability compared to mpCPAN-mpCNF and mpCNF-mpCPAN. This may be attributed to the absence of Nitrogen groups to trap the polysulfides through chemical bonds. mpCNF-mpCNF interlayer physically traps the polysulfides in the pores, which may eventually leach out into the electrolyte during discharge, or may also not get completely released for conversion to Sulfur during charging (hence, its poor Sulfur reutilization).

On the other hand, mpCPAN systems had a relatively lower N-content but increased mesopores, therefore allowing them to function effectively as both cathodes and interlayers. However, due to reduced Nitrogen content of mpCPAN the system mpCPAN-mpCPAN has the most superior performance, comparable to that of mpCNF-CPAN system. Presence of Nitrogen groups and mesopores in both cathodes and interlayers results in more effective polysulfide confinement and also show more promise for higher loading systems.

4. CONCLUSION

In summary, we have discussed the effects of using Mesoporous Carbon as a host for cyclic Nitrogen groups on battery performance. Eight systems utilizing Mesoporous/non Mesoporous Cyclized PAN fibers as cathode/interlayer were compared. It was found that non mesoporous Cyclized PAN was better utilized as an interlayer compared to a cathode. Another observation was that systems utilizing Cyclized PAN mesoporous fibers as both Cathode and interlayer

performed poorly compared to systems with no functional groups on either component. This was because of the significantly lower surface area and available active pores in mpCPAN, despite the ability of cyclic Nitrogen groups to chemically bond with Lithium Polysulfides. Therefore, introduction of Nitrogen groups in both cathode and interlayer with minimal loss of surface area and mesopores can ensure better polysulfide entrapment. For this purpose, an activation heat treatment step was carried out to obtain mesoporous cyclized PAN fibers. Despite lowered Nitrogen content, the increased mesopores showed a significant improvement in cell performance for all the Nitrogen containing systems, particularly mpCPAN-mpCPAN, relative to the reference mpCNF-mpCNF system. The heat treatment of Cyclized PAN fibers produced by conventional means, is a facile approach to optimize both N-content as well as surface area and mesopore content which are crucial for cathode performance.

ACKNOWLEDGEMENTS

This work was funded by EIC Labs (Cornell CCMR ICP No. M01-9124) and Axium Nano, LLC (Cornell OSP No. 80674). Electron Microscopy, optical spectroscopy and X-ray Spectroscopy were available through Cornell Center or Materials Research (CCMR- NSF Grant DMR-1719875).

REFERENCES

[1] D. Bresser, S. Passerini, B. Scrosati, Recent progress and remaining challenges in sulfur-based lithium secondary batteries – a review, Chem. Commun. 49 (2013) 10545. doi:10.1039/c3cc46131a.

[2] N.A. Cañas, K. Hirose, B. Pascucci, N. Wagner, K.A. Friedrich, R. Hiesgen, Investigations of lithium-sulfur batteries using electrochemical impedance spectroscopy, Electrochim. Acta. 97 (2013) 42–51. doi:10.1016/j.electacta.2013.02.101.

[3] A. Manthiram, S.-H. Chung, C. Zu, Lithium-Sulfur Batteries: Progress and Prospects, Adv. Mater. 27 (2015) 1980–2006. doi:10.1002/adma.201405115.

[4] Z.W. Seh, Y. Sun, Q. Zhang, Y. Cui, Designing high-energy lithium–sulfur batteries, Chem. Soc. Rev. 45 (2016) 5605–5634. doi:10.1039/C5CS00410A.

[5] Y.X. Yin, S. Xin, Y.G. Guo, L.J. Wan, Lithium-sulfur batteries: Electrochemistry, materials, and prospects, Angew. Chemie - Int. Ed. 52 (2013) 13186–13200. doi:10.1002/anie.201304762.

[6] A. Manthiram, Y. Fu, S. Chung, C. Zu, Y. Su, Rechargeable Lithium − Sulfur Batteries, (2014). doi:10.1021/cr500062v.

[7] A. Manthiram, S.-H. Chung, C. Zu, Lithium-Sulfur Batteries: Progress and Prospects, Adv. Mater. 27 (2015) 1980–2006. doi:10.1002/adma.201405115.

[8] B.P. Williams, Y.L. Joo, Tunable Large Mesopores in Carbon Nanofiber Interlayers for High-Rate Lithium Sulfur Batteries, J. Electrochem. Soc. 163 (2016) A2745–A2756. doi:10.1149/2.0931613jes.

[9] R. Elazari, G. Salitra, A. Garsuch, A. Panchenko, D. Aurbach, Sulfur-impregnated activated carbon fiber cloth as a binder-free cathode for rechargeable Li-S batteries, Adv. Mater. 23 (2011) 5641–5644. doi:10.1002/adma.201103274.

[10] N. Jayaprakash, J. Shen, S.S. Moganty, A. Corona, L.A. Archer, Porous hollow carbon@sulfur composites for high-power lithium-sulfur batteries, Angew. Chemie - Int. Ed. 50 (2011) 5904–5908. doi:10.1002/anie.201100637.

[11] L. Ji, M. Rao, H. Zheng, L. Zhang, Y. Li, W. Duan, J. Guo, E.J. Cairns, Y. Zhang, Graphene oxide as a sulfur immobilizer in high performance lithium/sulfur cells, J. Am. Chem. Soc. 133 (2011) 18522–18525. doi:10.1021/ja206955k.

[12] J. Schuster, G. He, B. Mandlmeier, T. Yim, K.T. Lee, T. Bein, L.F. Nazar, Spherical ordered mesoporous carbon nanoparticles with high porosity for lithium-sulfur batteries, Angew. Chemie - Int. Ed. 51 (2012) 3591–3595. doi:10.1002/anie.201107817.

[13]H. Wang, Y. Yang, Y. Liang, J.T. Robinson, Y. Li, A. Jackson, Y. Cui, H. Dai, Graphene-wrapped sulfur particles as a rechargeable lithium-sulfur battery cathode material with high capacity and cycling stability, Nano Lett. 11 (2011) 2644–2647. doi:10.1021/nl200658a.

[14] G. Zheng, Y. Yang, J.J. Cha, S.S. Hong, Y. Cui, Hollow carbon nanofiber-encapsulated sulfur cathodes for high specific capacity rechargeable lithium batteries, Nano Lett. 11 (2011) 4462–4467. doi:10.1021/nl2027684.

[15] Y.-S.S. Arumugam Manthiram, Lithium-Sulfur Batteries with Porous Carbon Interlayer Configurations, 5904 (2012) 8817. doi:10.1038/ncomms2163.

[16] T.Z. Hou, H.J. Peng, J.Q. Huang, Q. Zhang, B. Li, The formation of strong-couple interactions between nitrogen-doped graphene and sulfur/lithium (poly)sulfides in lithium-sulfur batteries, 2D Mater. 2 (2015). doi:10.1088/2053-1583/2/1/014011.

[17] F. Li, Y. Su, J. Zhao, Shuttle inhibition by chemical adsorption of lithium polysulfides in B and N co-doped graphene for Li–S batteries, Phys. Chem. Chem. Phys. 18 (2016) 25241–25248. doi:10.1039/C6CP04071C.

[18] L. Ma, H.L. Zhuang, S. Wei, K.E. Hendrickson, M.S. Kim, G. Cohn, R.G. Hennig, L.A. Archer, Enhanced Li-S batteries using amine-functionalized carbon nanotubes in the cathode, ACS Nano. 10 (2016) 1050–1059. doi:10.1021/acsnano.5b06373.

[19] Q. Pang, J. Tang, H. Huang, X. Liang, C. Hart, K.C. Tam, L.F. Nazar, A Nitrogen and Sulfur Dual-Doped Carbon Derived from Polyrhodanine@Cellulose for Advanced Lithium-Sulfur Batteries, Adv. Mater. 27 (2015) 6021–6028. doi:10.1002/adma.201502467.

[20] Z.W. Seh, H. Wang, P.-C. Hsu, Q. Zhang, W. Li, G. Zheng, H. Yao, Y. Cui, Facile synthesis of Li_2S–polypyrrole composite structures for high-performance Li2S cathodes, Energy Environ. Sci. 7 (2014) 672. doi:10.1039/c3ee43395a.

[21] L. Wang, Z. Yang, H. Nie, C. Gu, W. Hua, X. Xu, X. Chen, Y. Chen, S. Huang, A lightweight multifunctional interlayer of sulfur–nitrogen dual-doped graphene for ultrafast, long-life lithium–sulfur batteries, J. Mater. Chem. A. 4 (2016) 15343–15352. doi:10.1039/C6TA07027B.

[22] Q. Zeng, X. Leng, K.H. Wu, I.R. Gentle, D.W. Wang, Electroactive cellulose-supported graphene oxide interlayers for Li-S batteries, Carbon N. Y. 93 (2015) 611–619. doi:10.1016/j.carbon.2015.05.095.

[23] G. Zhou, E. Paek, G.S. Hwang, A. Manthiram, Long-life Li/polysulphide batteries with high sulphur loading enabled by lightweight three-dimensional nitrogen/sulphur-codoped graphene sponge, Nat. Commun. 6 (2015) 1–11. doi:10.1038/ncomms8760.

[24] M. Inagaki, Y. Yang, F. Kang, Carbon nanofibers prepared via electrospinning, Adv. Mater. 24 (2012) 2547–2566. doi:10.1002/adma.201104940.

[25] Q. Li, M. Liu, X. Qin, J. Wu, W. Han, G. Liang, D. Zhou, Y.-B. He, B. Li, F. Kang, Cyclized-polyacrylonitrile modified carbon nanofiber interlayers enabling strong trapping of polysulfides in lithium–sulfur batteries, J. Mater. Chem. A. 4 (2016) 12973–12980. doi:10.1039/C6TA03918A.

[26] J. Lee, B. Ko, J. Kang, Y. Chung, Y. Kim, W. Halim, J.H. Lee, Y.L. Joo, Facile and scalable fabrication of highly loaded sulfur cathodes and lithium–sulfur pouch cells via air-controlled electrospray, Mater. Today Energy. 6 (2017) 255–263. doi:10.1016/j.mtener.2017.11.003.

[27]C.F. Chen, A. Mistry, P.P. Mukherjee, Probing impedance and microstructure evolution in lithium-sulfur battery electrodes, J. Phys. Chem. C. 121 (2017) 21206–21216. doi:10.1021/acs.jpcc.7b07245.

[28] N.A. Cañas, K. Hirose, B. Pascucci, N. Wagner, K.A. Friedrich, R. Hiesgen, Investigations of lithium-sulfur batteries using electrochemical impedance spectroscopy, Electrochim. Acta. 97 (2013) 42–51. doi:10.1016/j.electacta.2013.02.101.

[29] S. Wei, L. Ma, K.E. Hendrickson, Z. Tu, L.A. Archer, Metal-Sulfur Battery Cathodes Based on PAN-Sulfur Composites, J. Am. Chem. Soc. 137 (2015) 12143–12152. doi:10.1021/jacs.5b08113.

[30] Z. Wang, Y. Dong, H. Li, Z. Zhao, H. Bin Wu, C. Hao, S. Liu, J. Qiu, X.W.D. Lou, Enhancing lithium-sulphur battery performance by strongly binding the discharge products on amino-functionalized reduced graphene oxide, Nat. Commun. 5 (2014) 1–8. doi:10.1038/ncomms6002.

[31] X. Liang, C. Hart, Q. Pang, A. Garsuch, T. Weiss, L.F. Nazar, A highly efficient polysulfide mediator for lithium-sulfur batteries, Nat. Commun. 6 (2015) 1–8. doi:10.1038/ncomms6682.

[32] L.F. Chen, X.D. Zhang, H.W. Liang, M. Kong, Q.F. Guan, P. Chen, Z.Y. Wu, S.H. Yu, Synthesis of nitrogen-doped porous carbon nanofibers as an efficient electrode material for supercapacitors, ACS Nano. 6 (2012) 7092–7102. doi:10.1021/nn302147s.

[33] J.F. Moulder, W.F. Stickle, P.E. Sobol, K.D. Bomben, Handbook of X-ray photoelectron spectroscopy: a reference book of standard spectra for identification and interpretation of XPS data, Surf. Interface Anal. (1992) 261. doi:9780962702624.

[34] T.Z. Hou, X. Chen, H.J. Peng, J.Q. Huang, B.Q. Li, Q. Zhang, B. Li, Design Principles for Heteroatom-Doped Nanocarbon to Achieve Strong Anchoring of Polysulfides for Lithium–Sulfur Batteries, Small. (2016) 3283–3291. doi:10.1002/smll.201600809.

[35] T.Z. Hou, H.J. Peng, J.Q. Huang, Q. Zhang, B. Li, The formation of strong-couple interactions between nitrogen-doped graphene and sulfur/lithium (poly)sulfides in lithium-sulfur batteries, 2D Mater. 2 (2015). doi:10.1088/2053-1583/2/1/014011.

CHAPTER 3

UTILIZING NITROGEN FUNCTIONALIZED CARBON NANOFIBERS PRODUCED BY ELECTROSPINNING UREA-POLYACRYLONITRILE PRECURSOR AS LITHIUM SULFUR INTERLAYERS AND CATHODES

1. INTRODUCTION

As demand for energy increases, there is a growing need for clean, efficient and cost effective renewable energy sources and reduce the usage of fossil fuels. Lithium Sulfur batteries have a high theoretical energy density of 2600 Wh/kg and a specific capacity of 1675 mAh/g. Sulfur is abundantly available and is environmentally benign [1-3]. All these reasons make Lithium Sulfur batteries among one of the most promising next generation rechargeable batteries. However, Lithium Sulfur batteries face several challenges in performance that need to be resolved before they can be commercially viable. One of these is the dissolution of higher order polysulfides into the electrolyte, which makes it difficult to recover them as Lithium Sulfide precipitate on the cathode at the end of discharge cycle, leading to loss of active material and low capacity. Another challenge is the polysulfide shuttle effect, when the higher order polysulfides migrate to the anode, get reduced to Li_2S and migrate back to the cathode to get reoxidized. The insulating nature of Sulfur and Lithium Sulfide also adds to the cell resistance [4-7].

Several efforts have been made to combat the technical issues mentioned above. It has been found that several types of carbon nanomaterials such as microporous carbon, mesoporous carbon, hierarchical porous carbon, carbon black, hollow carbon spheres, CNTs, CNFs, reduced graphene oxide and graphene can improve cell performance. These porous carbons can contain the active material, constrain the dissolved polysulfides, and accelerate charge/electron transport [8-14]. Manthiram et al introduced the concept of inserting an

interlayer between the cathode and separator to acts as a polysulfide entrapper and enhance the reutilization of trapped material. However, despite the improved performance, this acts as a temporary solution since the interlayer acts as only a physical barrier and the polysulfides can eventually leach out to the electrolyte [15].

To ensure more permanent constraining of polysulfides, chemical modification of active hosts surface are also effective in reducing shuttle effect and improving cycle performance. Introduction of doping elements like Nitrogen, Sulfur, Phosphorus, Boron have been shown formation of strong chemical bonds between the polysulfides and these elements[16,17]. Nitrogen doping has been done by introducing electron-rich functional groups like Amines, polypyrrole, pyrroles, pyridines and has been found to be effective in assisting mesoporous carbon in suppressing polysulfide shuttling effect through Lewis Acid-Base interactions with polysulfides[18-23].

Incorporation of Nitrogen into carbon susbtrates like Carbon Nanotubes (CNTs), Carbon Nanofibers (CNFs) has been found to be beneficial in improving electrochemical and electrocatalytic activity of Metal-ion batteries, fuel cells and super capacitors.

Wang *et al* reported the effect of addition of Nitrogen sources like Melamine, Aniline, Urea and Polyaniline to Polyacrylonitrile (PAN) precursors which were used for electrospinning [24]. Addition of these Nitrogen sources in varying ratios with respect to PAN increased the nitrogen content of the electrospun Carbon nanofibers. Carbonization of the nanofibers incorporated Pyridinic and Pyrollic Nitrogen groups which resulted in significant improvement in electrocatalytic activity of fuel cells. Xu *et al* reported a facile synthesis of highly doped CNFs for application in Potassium-ion batteries [25]. A polypyrrole precursor was prepared by oxidation of pyrrole monomers in the presence of Ammonium Persulfate reagent. The precursor was carbonized at varying temperatures to obtain CNFs doped with pyrollic Nitrogen and utilized as Anode. the resulting CNFs had a 13.8% Nitrogen content. It

was found that with increasing carbonization temperature from 650-1100^{0}C, the Nitrogen content reduced, resulting in reduction of specific capacity.

Another study by Zhang *et al*, reported the addition of urea to PAN precursors in varying concentrations for electrospinning [26]. The carbonization of the electrospun nanofibers introduced C-N and C=N bonds due to the presence of Pyridinic and Pyrollic Nitrogen groups, which increased their conductivity. The Nitrogen content increased from 11.31-19.06% with increasing Urea content from 10-30wt% in the PAN precursor. Chen *et al* reported a one step, process for N-doping multiwalled CNTs utilized as Oxidation Reduction Reaction(ORR) catalyst support [27]. Ammonium Hydroxide was used as a Nitrogen source for doping CNTs in a hydrothermal reaction at 180^{0}C for 12 hours. This synthesis has several advantages: cost effective, mild reaction conditions and also maintains the high BET surface area and original multiwalled structure of the CNTs. However it results in a low Nitrogen content (1.32 at%) . Another interesting technique of using Polypyrrole doped carbon was reported by Guo *et al* [28]. PAN was functionalized with Polypyrrole by in-situ polymerization, where the nanofibers were immersed in a Pyrrole monomer solution which were oxidized to Polypyrrole in the presence of $FeCl_3$. The as treated fibers were carbonized and a Nitrogen content of 12.53at% was reported. Gan *et al* also utilized Polypyrrole as a nitrogen dopant for CNF in capacitors [29]. In this work, CNFs obtained after electrospinning and carbonization were coated with Graphene and Polypyrrole by electrodeposition. The graphene/Polypyrrole coated CNF resulted in increased conductivity and improved rate performance.

Wu *et al* reported a facile method of functionalizing carbon nanofibers for improving ORR catalytic activity in fuel cells [30]. They electrospun interconnected Fe-N/C nanofiber networks using Polyvinylpyrollidone and Iron acetylacetonate as precursors . The Nitrogen

doping created Pyridine, Pyrolle, Graphitic and Pyridinic Oxide groups in the interconnected fibers. Electron transport between the fibers was enhanced resulting in improved conductivity. Gu et al reported a two step process to functionalize Graphene with N and P and utilize it as an interlayer [31]. Phosphorus was incorporated into the Graphene matrix by thermal annealing using Triphenylphosphine as a precursor. Nitrogen doping was done by employing a hydrothermal reaction with ammonia solution as the precursor. The resulting composition of N,P in graphene was found to be 4.48% and 1.93% respectively. The functionalized graphene was coated onto a separator and utilized as a polysulfide blocking layer.

In this paper, we study and compare the results of functionalizing mesoporous Carbon cathodes and interlayers with electron rich Nitrogen groups. Mesoporous Carbon nanofiber webs were synthesized by gas assisted electrospinning of Polyacrylonitrile/Urea precursor solutions , and used as both cathode and interlayer in our system. Cathodes were prepared by electrospraying Sulfur onto Mesoporous Carbon, a facile technique which can be used to created higher loading Sulfur electrodes . The surface chemistry of these mesoporous fibers was modified by introducing cyclic Nitrogen groups and heat treatments . They were then utilized as cathodes and interlayers to test the effects of adding cyclic Nitrogen groups on cell performance .

2. EXPERIMENTAL

2.1 Synthesis of Mesoporous Carbon Nanofiber web (mpCNF)

Polyacrylonitrile (PAN) (mw=150,000 from Sigma Aldrich) and Poly(methyl methylacrylate) (PMMA) were dissolved in dimethylformamide (DMF) to a 12 wt% polymer content, by stirring at 65^0C for 12 hours [32]. The nanofibers were prepared by gas assisted electrospinning at 15kV, 30 cms distance from the collector at a 0.075ml/min flow rate. An 18 gauge stainless steel needle was used for electrospinning. The nanofibers were stabilized in air

at 280^{0}C for 2 hours, carbonized in Nitrogen at 900^{0}C for 2 hours and activated in Carbon Dioxide at 900^{0}C for 2 hours.

2.2 Synthesis of mesoporous Nitrogen doped polyacrylonitrile modified CNF fibers (mpNCNF)

Polyacrylonitrile (PAN) (mw=150,000 from Sigma Aldrich), Urea and Poly(methyl methylacrylate) (PMMA) were dissolved in dimethylformamide (DMF) to a 12 wt% polymer content (PAN:PMMA:Urea=60:30:10, by weight), by stirring at 65^{0}C for 12 hours.The nanofibers were prepared by gas assisted electrospinning at 15kV, 30 cms distance from the collector at a 0.075ml/min flow rate and 20% Relative Humidity. An 18 gauge stainless steel needle was used for electrospinning. The nanofibers that were utilized as interlayers were stabilized in air at 280^{0}C for 2 hours and carbonized in Nitrogen at 700^{0}C for 2 hours(mpNCNF-700). mpNCNF that were utilized as electrodes were carbonized in Nitrogen at 900^{0}C for 2 hours underwent and activated in Carbon Dioxide at 700^{0}C for 1 hour (mpNCNF-900).

2.3 Synthesis of mpCNF and mpNCNF electrodes

The mpNCNF-900 and mpCNF electrodes were synthesized by air controlled electrospraying [33]. Sublimed sulfur(Spectrum Chemical Mfg.Corp) and Ketjen Black EC-600JD(KB)(AzkoNobel) solution were dispersed in CS_2 to obtain a composition of 97% Sulfur and 3% Ketjen Black . The solution was stirred for 3 hours and sonicated for 30 minutes before electrospraying on mpCNF and mpNCNF-900 webs at 15kV, 10 cms distance from the collector at 0.08ml/min flow rate. An 18 gauge stainless steel needle was used for air controlled electrospraying**.** Electrospraying was carried out until the target Sulfur loading was deposited on the cathode. Cathodes with Sulfur loading of 1.1mg/cm^2 were used for testing. Sulfur content of the substrates was 14.3%.

2.4 Material Characterization

The pore size distribution analysis was performed on a Micrometrics Gemini VII 2390t in liquid Nitrogen with the Brunauer, Emmett and Teller (BET) method. Samples were degassed under nitrogen at 300^0C for at least 3 hours. The scanning electron microscope (SEM) images were taken by a TESCAN Mira3 Field Emission SEM and Zeiss Gemini 500 SEM . The Fourier Transform infrared (FTIR) spectra of mpCNF and mpCPAN was carried out using a Bruker-Hyperion FT-IR Microscope at ambient temperature. X-ray Photoelectron spectroscopy (XPS) of mpNCNF and mpCNF before and after cycling was used to obtain chemical bonding information and elemental analysis.

2.5 Electrochemical Characterization

The interlayers and substrates were cut into discs of diameter 15 mm from the nanofiber mat. CR2032 coin cells were assembled using Sulfur deposited mpCPAN/mpCNF (5.5mg/cm^2) as cathodes, Lithium metal (same diameter as cathode) as anode, mpCPAN/mpCNF (8.2mg/cm^2) as interlayers, a 25 micron thick Celgard separator and an electrolyte of 1M lithium bis-(trifluroromethanesulfone)imide and 0.2M $LiNO_3$ in 1,2-dioxolane/1,2-dimethoxyethane (v/v=1:1). EIS measurements were carried out using a Solartorn Cell Test System model 1470E potentiostat between frequencies 0.01-100kHz.

3. RESULTS AND DISCUSSION

XPS and FT-IR scans were used to characterize the surfaces of mpCNF, mpNCNF-700 and mpNCNF-900 and confirm the presence of Nitrogen groups in mpNCNF . XPS survey scan of mpCNF is presented in Fig 1 (a). In the case of mpCNF, we see 2 prominent peaks for C 1s at 285eV and O 1s at 532eV. For XPS survey scans of mpNCNF-700 and mpNCNF-900, we see a third prominent peak for N 1s at 400eV. Fig 1(b) shows the deconvoluted N 1s signals with 2 peaks for pyridine and pyrrole at 398eV and 399.9 eV respectively[34,35] .

(a)

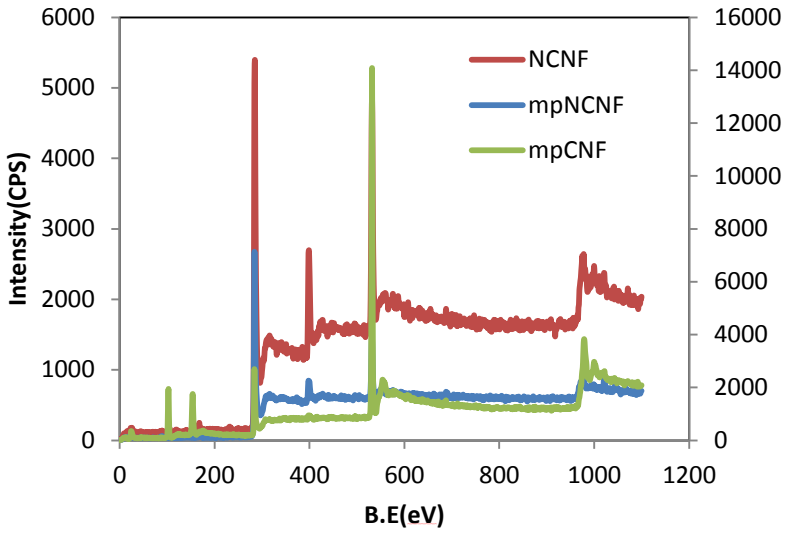
6000
5000
4000
3000
2000
1000
0
16000
14000
12000
10000
8000
6000
4000
2000
0
0
200
400
600
800
1000
1200
Intensity(CPS)
B.E(eV)
NCNF
mpNCNF
mpCNF

(b)

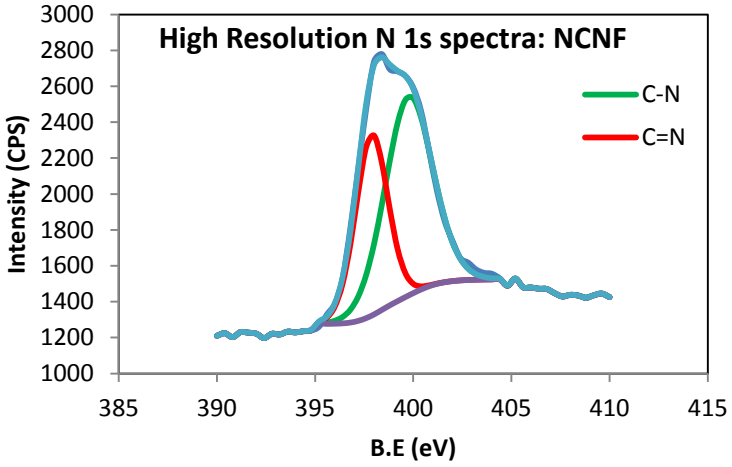
High Resolution N 1s spectra: NCNF
3000
2800
2600
2400
2200
2000
1800
1600
1400
1200
1000
385
390
395
400
405
410
415
Intensity (CPS)
B.E (eV)
C-N
C=N

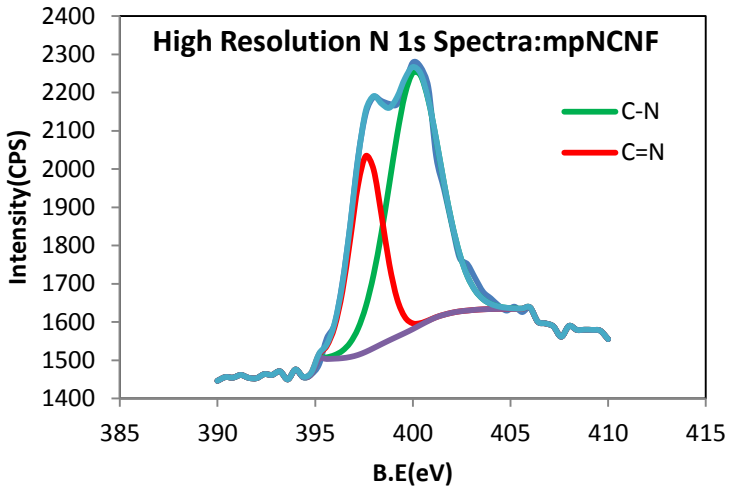

Fig 1 (a) XPS Survey Scan of mpCNF,NCNF and mpNCNF (b) High resolution N 1s spectra of NCNF and mpNCNF

FTIR spectra of mpnCNF-700 and mpNCNF-900 in Fig 2 shows absorbance bands at approximately 1041and 1097 cm^{-1} which represent C-N stretching. The peak at 1562cm^{-1} represents the vibration of combined C=C and C=N and the peak around 1360cm^{-1} is for C-C stretching [34,35].

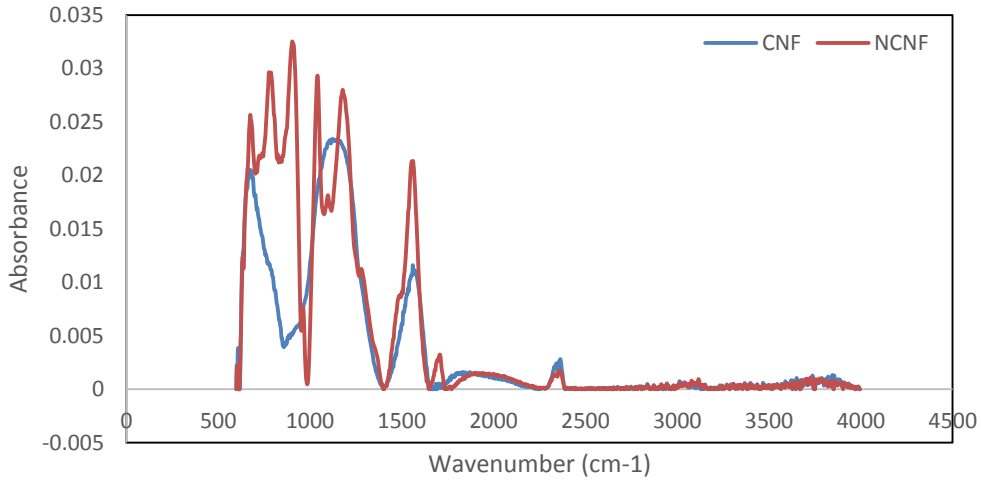

Fig 2. FTIR Scan of mpCNF and mpNCNF

SEM and EDS mapping images of mpCNF ,mpNCNF and NCNF are shown in **Fig 3**. NCNF fibers have a rough surface morphology compared to mpCNF and mpNCNF indicative of effective surface modification. EDS mapping images show that elemental Nitrogen is uniformly distributed along mpNCNF and NCNF fibers.

(a)

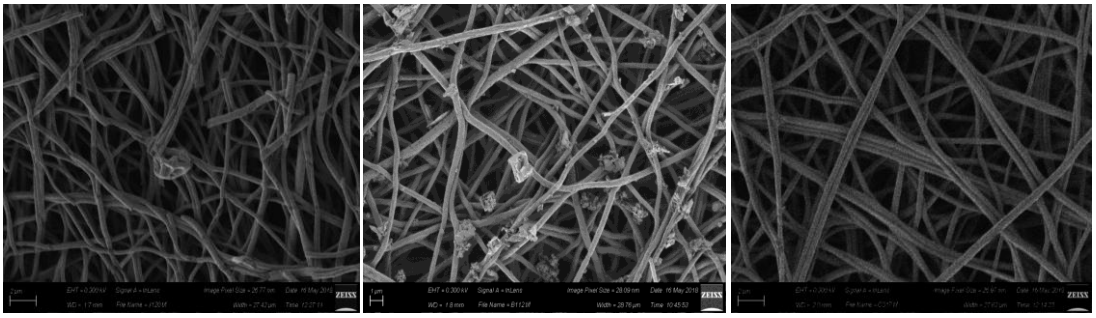

(b)

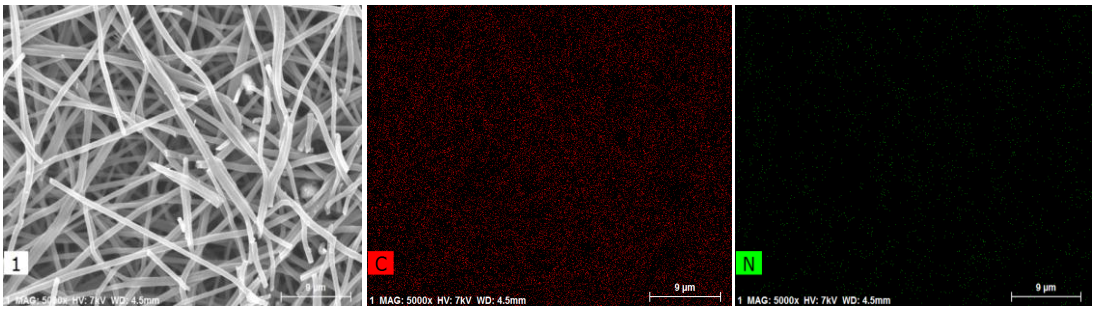

(c)

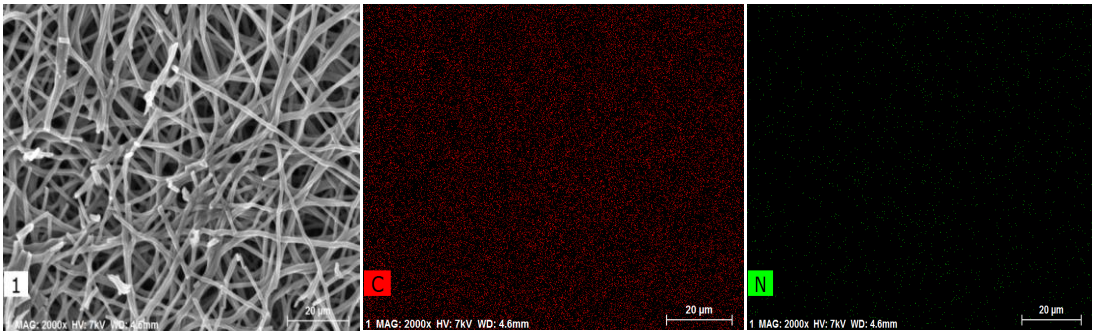

Fig 3. (a) SEM Images of mpCNF,NCNF and mpNCNF (b) EDS Mapping Images of mpNCNF (c) EDS Mapping Images of NCNF

The BET surface area of mpCNF at 504.28 m^2/g is higher than that of NCNF and mpNCNF at 42m^2/g and 298.08m^2/g respectively. The pore size distribution in **Fig 4** shows the presence of mesopores in mpCNF, activated mpNCNF and non activated mpNCNF. An improvement in mesopore distribution was observed after activation of mpNCNF.

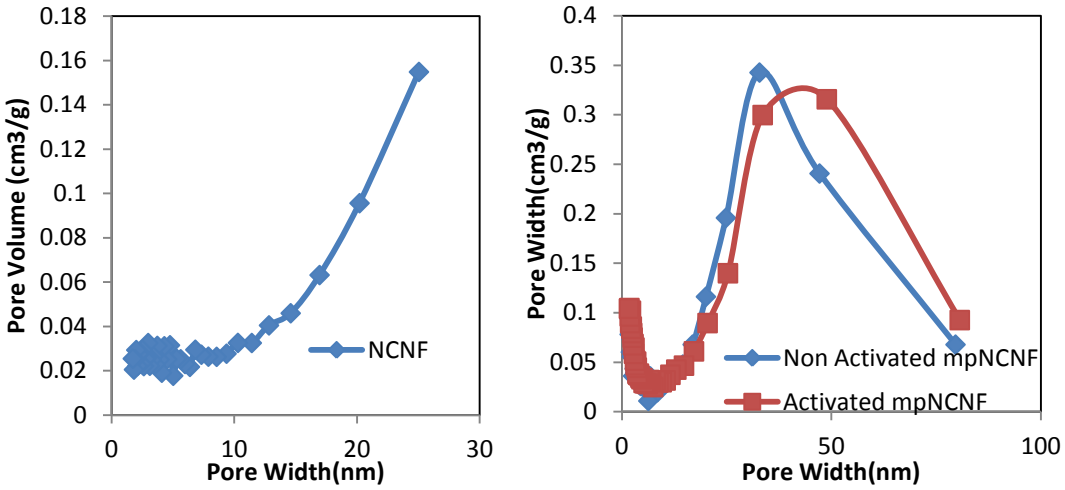

Fig 4. BJH Pore size distribution of NCNF and mpNCNF

To analyze the effects of utilizing N-doped carbon nanofibers as electrode materials and interlayers, electrochemical tests were carried out for four combinations of systems:

- mpCNF cathode and mpCNF interlayer (mpCNF-mpCNF)
- mpCNF cathode and mpNCNF-700 interlayer (mpCNF-NCNF)
- mpNCNF-900 cathode and mpCNF interlayer (mpNCNF-mpCNF)
- mpNCNF-900 cathode and mpNCNF-700 interlayer (mpNCNF-NCNF)

Cycle tests were carried out at 0.3C for 100 cycles using sulfur loading 1.1mg/cm^2. Cycle and rate capability tests are shown in **Fig 5(a) and Fig 5(b)**. From the cycle performance, a significant improvement in cycle stability is observed when at least one component is Nitrogen doped. mpNCNF-NCNF and mpCNF-NCNF systems have better cycle performance compared to mpNCNF-mpCNF and mpCNF-mpCNF systems. This can be attributed to the

higher Nitrogen content in the first two systems as compared to mpNCNF-mpCNF and mpCNF-mpCNF systems, resulting in more effective polysulfide entrapment. In the rate capability performance, mpNCNF-NCNF and mpCNF-NCNF, a high specific capacity of 1271mAh/g and 1197mAh/g even at a high current density of 2C was observed, which can be attributed to a synergy between high mesopore content for easy ion and electrolyte diffusion, and high Nitrogen content for improved conductivity and efficient polysulfide confinement[36]

(a)

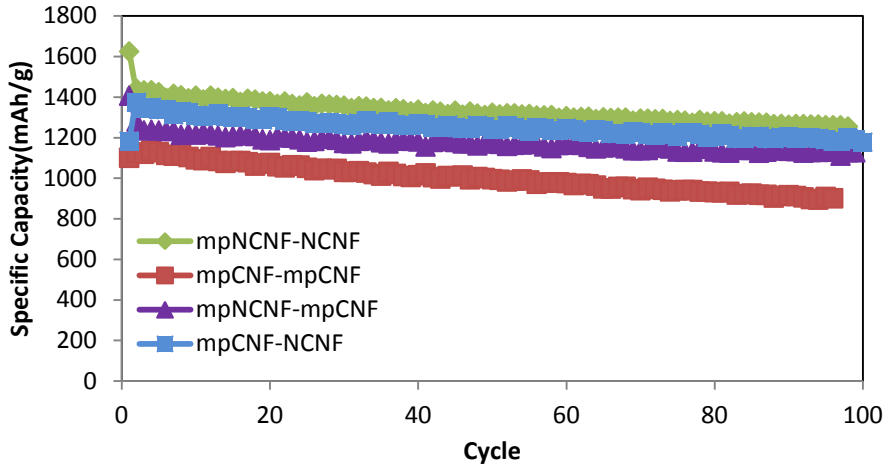

(b)

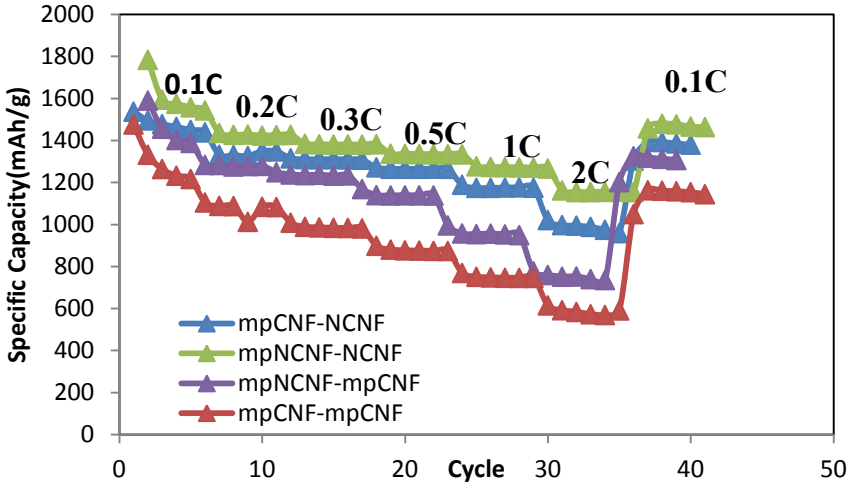

Fig 5. (a)Cycle Performances of 4 systems at 0.3C, 1.2mg/cm^2 S-Loading (b) Rate Capability Tests at 1.2mg/cm^2 S-loading

Electrochemical impedance spectroscopy of fresh cells and cells after cycle performance were carried out . The EIS spectra in Fig 6 (a),(b) shows that systems with at least one Nitrogen doped component have a lower charge transfer resistance 8Ω(mpNCNF-NCNF) and 10 Ω(mpNCNF-mpCNF and mpCNF-NCNF) compared to 11 Ω for mpCNF-mpCNF system. After 100 cycles, the charge transfer resistance is reduced but in the cases of mpCNF-mpCNF and mpNCNF-mpCNF, a second semi-circle appeared in the high frequency range which can be attributed to the formation of discharge product Li_2S precipitate film [37,38]. Since these systems have mpCNF as an interlayer, it is possible that though polysulfides were deposited in between the fibers, they could not be reutilized efficiently during future charging and discharging cycles.

(a)

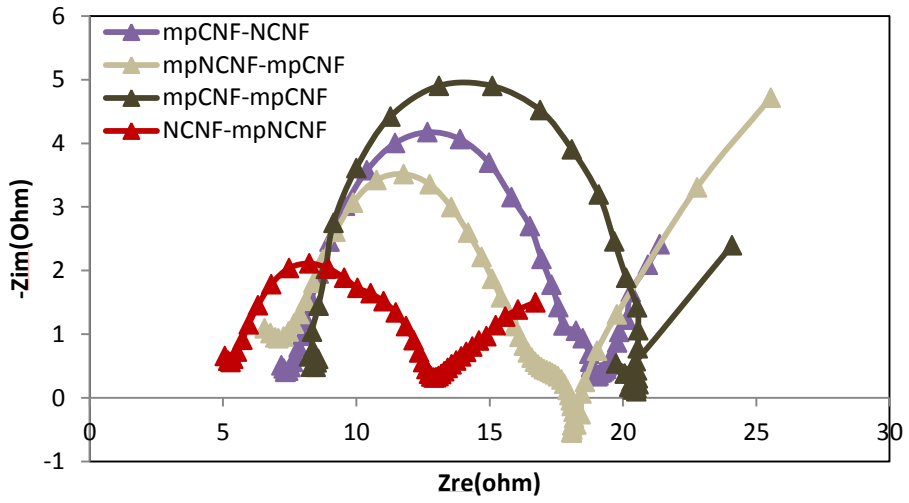

(b)

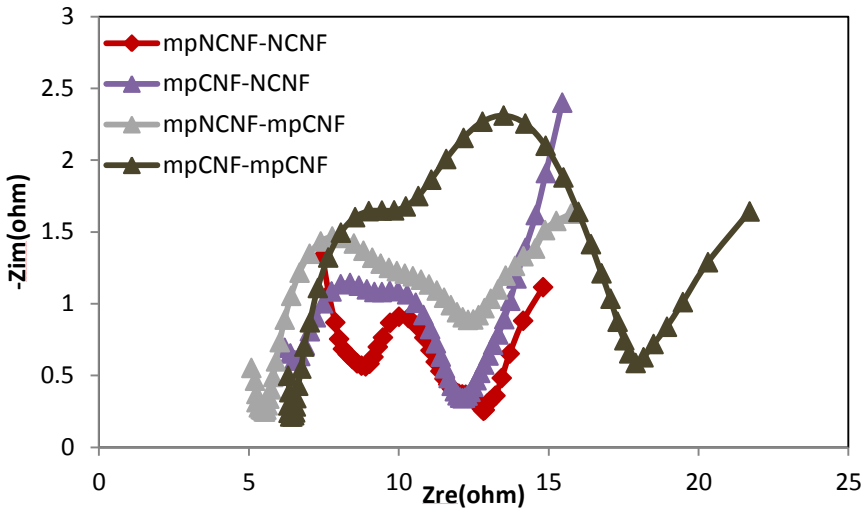

Fig 6. (a)EIS Spectra of Fresh Cells (b) EIS Spectra of cells after 100 cycles

Post mortem XPS analysis of cathodes and interlayers of fully discharged cells was carried to understand the interactions between polysulfide and Nitrogen groups. In **Fig 7**, High resolution S 2p spectra of N-doped cathodes and interlayers was examined.

(a) (b)

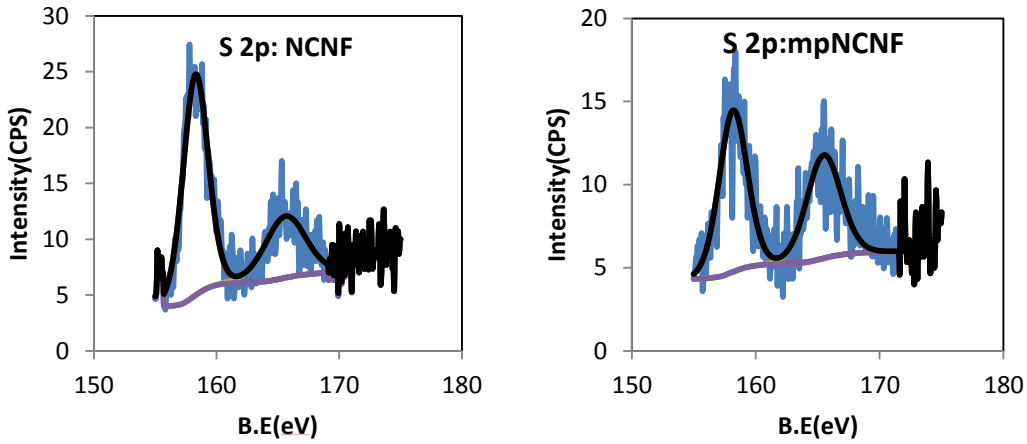

Fig 7. High Resolution S 2p spectra of (a)mpNCNF and (b)NCNF after discharge

Two significant peaks are generally observed at 165.39eV and 159.4 eV, corresponding to Sulfate peaks due to air and moisture sensitivity of Li_2S [39] and Li_2S precipitate [39,40]. The Pyridinic and Pyrollic groups donate an electron to elemental sulfur . This reaction also explains why the sulfur peaks shift to lower binding energy than the literature value: the electron donation from the Nitrogen groups shifts the electron cloud towards Nitrogen, thereby reducing the energy required for the S 2p electron to be knocked out by the X-rays [41,42]. On comparing the peaks corresponding to polysulfides, it appears that the peak intensity is significantly higher for NCNF interlayers compared to mpNCNF cathodes. This may be due to the much higher Nitrogen content of the interlayers which results in higher polysulfide confinement ability.

High resolution N 1s spectra of N-doped cathodes and interlayers were also analyzed, as shown in **Fig 8**. Two peaks are observed: one corresponding to the cyclic Nitrogen group and the second is a peak shifted towards a lower binding energy of 396.6eV, corresponding to Li-N interactions.

(a) (b)

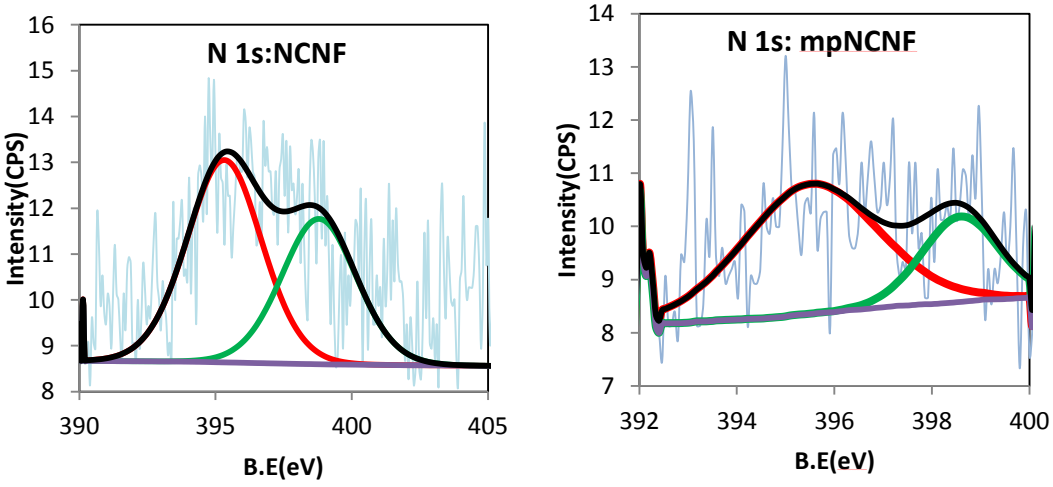

Fig 8. High Resolution N 1s spectra of (a) mpNCNF and (b)NCNF after discharge

When comparing the intensities of shifted peaks to the cyclic Nitrogen group peaks, it appears that for NCNF interlayers, the shifted peaks have a significantly higher intensity relative to the original ones. In contrast, for mpNCNF electrodes, both peaks appear to be of comparable intensities. This implies that NCNF has a much higher utilization of Nitrogen groups for polysulfide interactions than mpNCNF, possible due to its dual role as both a physical and chemical barrier for polysulfides. These results can also be attributed to the higher Nitrogen content of NCNF interlayers and could explain the relatively poor performance of mpNCNF-mpCNF system.

4. CONCLUSIONS

We have analyzed the combined effects of Nitrogen doping and improving mesopore distribution on limiting polysulfide dissolution and thereby, improving cell performance. It was found that even low concentrations of Nitrogen led to lower capacity fading and improved rate capability. However, the system with mesoporous, low Nitrogen content electrode and a non mesoporous, high Nitrogen content interlayer appeared to be the most effective in confining soluble higher order polysulfides to the carbon nanofiber surfaces. This was attributed to improved conductivity, reduced charge transfer resistance and an optimal Nitrogen content in the overall system to trap polysulfides without sacrificing mesopores, which are crucial for Sulfur deposition. Therefore, it can be concluded that the addition of Urea as a nitrogen source to PAN precursor solutions is a facile approach to produce relatively high concentration, Nitrogen doped mesoporous carbon nanofibers as electrodes and interlayers.

5. ACKNOWLEDGEMENTS

This work was funded by EIC Labs (Cornell CCMR ICP No. M01-9124) and Axium Nano, LLC (Cornell OSP No. 80674). Electron Microscopy, optical spectroscopy and X-ray

Spectroscopy were available through Cornell Center or Materials Research (CCMR- NSF Grant DMR-1719875)

REFERENCES

[1] D. Bresser, S. Passerini, B. Scrosati, Recent progress and remaining challenges in sulfur-based lithium secondary batteries – a review, Chem. Commun. 49 (2013) 10545. doi:10.1039/c3cc46131a.

[2] N.A. Cañas, K. Hirose, B. Pascucci, N. Wagner, K.A. Friedrich, R. Hiesgen, Investigations of lithium-sulfur batteries using electrochemical impedance spectroscopy, Electrochim. Acta. 97 (2013) 42–51. doi:10.1016/j.electacta.2013.02.101.

[3] A. Manthiram, S.-H. Chung, C. Zu, Lithium-Sulfur Batteries: Progress and Prospects, Adv. Mater. 27 (2015) 1980–2006. doi:10.1002/adma.201405115.

[4] Z.W. Seh, Y. Sun, Q. Zhang, Y. Cui, Designing high-energy lithium–sulfur batteries, Chem. Soc. Rev. 45 (2016) 5605–5634. doi:10.1039/C5CS00410A.

[5] Y.X. Yin, S. Xin, Y.G. Guo, L.J. Wan, Lithium-sulfur batteries: Electrochemistry, materials, and prospects, Angew. Chemie - Int. Ed. 52 (2013) 13186–13200. doi:10.1002/anie.201304762.

[6] A. Manthiram, Y. Fu, S. Chung, C. Zu, Y. Su, Rechargeable Lithium − Sulfur Batteries, (2014). doi:10.1021/cr500062v.

[7] A. Manthiram, S.-H. Chung, C. Zu, Lithium-Sulfur Batteries: Progress and Prospects, Adv. Mater. 27 (2015) 1980–2006. doi:10.1002/adma.201405115.

[8] B.P. Williams, Y.L. Joo, Tunable Large Mesopores in Carbon Nanofiber Interlayers for High-Rate Lithium Sulfur Batteries, J. Electrochem. Soc. 163 (2016) A2745–A2756. doi:10.1149/2.0931613jes.

[9] R. Elazari, G. Salitra, A. Garsuch, A. Panchenko, D. Aurbach, Sulfur-impregnated activated carbon fiber cloth as a binder-free cathode for rechargeable Li-S batteries, Adv. Mater. 23 (2011) 5641–5644. doi:10.1002/adma.201103274.

[10] N. Jayaprakash, J. Shen, S.S. Moganty, A. Corona, L.A. Archer, Porous hollow carbon@sulfur composites for high-power lithium-sulfur batteries, Angew. Chemie - Int. Ed. 50 (2011) 5904–5908. doi:10.1002/anie.201100637.

[11] L. Ji, M. Rao, H. Zheng, L. Zhang, Y. Li, W. Duan, J. Guo, E.J. Cairns, Y. Zhang, Graphene oxide as a sulfur immobilizer in high performance lithium/sulfur cells, J. Am. Chem. Soc. 133 (2011) 18522–18525. doi:10.1021/ja206955k.

[12] J. Schuster, G. He, B. Mandlmeier, T. Yim, K.T. Lee, T. Bein, L.F. Nazar, Spherical ordered mesoporous carbon nanoparticles with high porosity for lithium-sulfur batteries, Angew. Chemie - Int. Ed. 51 (2012) 3591–3595. doi:10.1002/anie.201107817.

[13] H. Wang, Y. Yang, Y. Liang, J.T. Robinson, Y. Li, A. Jackson, Y. Cui, H. Dai, Graphene-wrapped sulfur particles as a rechargeable lithium-sulfur battery cathode material with high capacity and cycling stability, Nano Lett. 11 (2011) 2644–2647. doi:10.1021/nl200658a.

[14] G. Zheng, Y. Yang, J.J. Cha, S.S. Hong, Y. Cui, Hollow carbon nanofiber-encapsulated sulfur cathodes for high specific capacity rechargeable lithium batteries, Nano Lett. 11 (2011) 4462–4467. doi:10.1021/nl2027684.

[15] Y.-S.S. Arumugam Manthiram, Lithium-Sulfur Batteries with Porous Carbon Interlayer Configurations, 5904 (2012) 8817. doi:10.1038/ncomms2163.

[16] T.Z. Hou, H.J. Peng, J.Q. Huang, Q. Zhang, B. Li, The formation of strong-couple interactions between nitrogen-doped graphene and sulfur/lithium (poly)sulfides in lithium-sulfur batteries, 2D Mater. 2 (2015). doi:10.1088/2053-1583/2/1/014011.

[17] F. Li, Y. Su, J. Zhao, Shuttle inhibition by chemical adsorption of lithium polysulfides in B and N co-doped graphene for Li–S batteries, Phys. Chem. Chem. Phys. 18 (2016) 25241–25248. doi:10.1039/C6CP04071C.

[18] L. Ma, H.L. Zhuang, S. Wei, K.E. Hendrickson, M.S. Kim, G. Cohn, R.G. Hennig, L.A. Archer, Enhanced Li-S batteries using amine-functionalized carbon nanotubes in the cathode, ACS Nano. 10 (2016) 1050–1059. doi:10.1021/acsnano.5b06373.

[19] Q. Pang, J. Tang, H. Huang, X. Liang, C. Hart, K.C. Tam, L.F. Nazar, A Nitrogen and Sulfur Dual-Doped Carbon Derived from Polyrhodanine@Cellulose for Advanced Lithium-Sulfur Batteries, Adv. Mater. 27 (2015) 6021–6028. doi:10.1002/adma.201502467.

[20] Z.W. Seh, H. Wang, P.-C. Hsu, Q. Zhang, W. Li, G. Zheng, H. Yao, Y. Cui, Facile synthesis of Li_2S–polypyrrole composite structures for high-performance Li2S cathodes, Energy Environ. Sci. 7 (2014) 672. doi:10.1039/c3ee43395a.

[21] L. Wang, Z. Yang, H. Nie, C. Gu, W. Hua, X. Xu, X. Chen, Y. Chen, S. Huang, A lightweight multifunctional interlayer of sulfur–nitrogen dual-doped graphene for ultrafast, long-life lithium–sulfur batteries, J. Mater. Chem. A. 4 (2016) 15343–15352. doi:10.1039/C6TA07027B.

[22] Q. Zeng, X. Leng, K.H. Wu, I.R. Gentle, D.W. Wang, Electroactive cellulose-supported graphene oxide interlayers for Li-S batteries, Carbon N. Y. 93 (2015) 611–619. doi:10.1016/j.carbon.2015.05.095.

[23] G. Zhou, E. Paek, G.S. Hwang, A. Manthiram, Long-life Li/polysulphide batteries with high sulphur loading enabled by lightweight three-dimensional nitrogen/sulphur-codoped graphene sponge, Nat. Commun. 6 (2015) 1–11. doi:10.1038/ncomms8760.

[24] S. Wang, C. Dai, J. Li, L. Zhao, Z. Ren, Y. Ren, Y. Qiu, J. Yu, The effect of different nitrogen sources on the electrocatalytic properties of nitrogen-doped electrospun carbon nanofibers for the oxygen reduction reaction, Int. J. Hydrogen Energy. 40 (2015) 4673–4682. doi:10.1016/j.ijhydene.2015.02.031.

[25] Y. Xu, C. Zhang, M. Zhou, Q. Fu, C. Zhao, M. Wu, Y. Lei, Highly nitrogen-doped carbon nanofibers as potassium-ion battery anodes with superior rate capability and cyclability, Nat. Commun. (n.d.) 1–29. doi:10.1038/s41467-018-04190-z.

[26] C. Chen, Y. Lu, Y. Ge, J. Zhu, H. Jiang, Y. Li, Y. Hu, X. Zhang, Synthesis of Nitrogen-Doped Electrospun Carbon Nanofibers as Anode Material for High-Performance Sodium-Ion Batteries, Energy Technol. 4 (2016) 1440–1449. doi:10.1002/ente.201600205.

[27] L. Chen, X. Cui, Y. Wang, M. Wang, F. Cui, C. Wei, W. Huang, Z. Hua, L. Zhang, J. Shi, One-step hydrothermal synthesis of nitrogen-doped carbon nanotubes as an efficient electrocatalyst for oxygen reduction reactions, Chem. - An Asian J. 9 (2014) 2915–2920. doi:10.1002/asia.201402334.

[28] J. Guo, J. Liu, H. Dai, R. Zhou, T. Wang, C. Zhang, S. Ding, H. guo Wang, Nitrogen doped carbon nanofiber derived from polypyrrole functionalized polyacrylonitrile for applications in lithium-ion batteries and oxygen reduction reaction, J. Colloid Interface Sci. 507 (2017) 154–161. doi:10.1016/j.jcis.2017.07.117.

[29] J.K. Gan, Y.S. Lim, A. Pandikumar, N.M. Huang, H.N. Lim, Graphene/polypyrrole-coated carbon nanofiber core–shell architecture electrode for electrochemical capacitors, RSC Adv. 5 (2015) 12692–12699. doi:10.1039/C4RA14922J.

[30] N. Wu, Y. Wang, Y. Lei, B. Wang, C. Han, Y. Gou, Q. Shi, Electrospun interconnected Fe-N / C nanofiber networks as efficient electrocatalysts for oxygen reduction reaction in acidic media, Nat. Publ. Gr. (2015) 1–9. doi:10.1038/srep17396.

[31] L.L. Beijing, C. Science, Porous nitrogen and phosphorous dual doped graphene blocking layer for high performance Li–S batteries, (2016). doi:10.1039/C5TA04255K.

[32] M. Inagaki, Y. Yang, F. Kang, Carbon nanofibers prepared via electrospinning, Adv. Mater. 24 (2012) 2547–2566. doi:10.1002/adma.201104940.

[33] J. Lee, B. Ko, J. Kang, Y. Chung, Y. Kim, W. Halim, J.H. Lee, Y.L. Joo, Facile and scalable fabrication of highly loaded sulfur cathodes and lithium–sulfur pouch cells via air-controlled electrospray, Mater. Today Energy. 6 (2017) 255–263. doi:10.1016/j.mtener.2017.11.003.

[34] G. Zhou, E. Paek, G.S. Hwang, A. Manthiram, Long-life Li/polysulphide batteries with high sulphur loading enabled by lightweight three-dimensional nitrogen/sulphur-codoped graphene sponge, Nat. Commun. 6 (2015) 1–11. doi:10.1038/ncomms8760.

[35] Q. Li, M. Liu, X. Qin, J. Wu, W. Han, G. Liang, D. Zhou, Y.-B. He, B. Li, F. Kang, Cyclized-polyacrylonitrile modified carbon nanofiber interlayers enabling strong trapping of polysulfides in lithium–sulfur batteries, J. Mater. Chem. A. 4 (2016) 12973–12980. doi:10.1039/C6TA03918A.

[36] C. Tang, Q. Zhang, M.Q. Zhao, J.Q. Huang, X.B. Cheng, G.L. Tian, H.J. Peng, F. Wei, Nitrogen-doped aligned carbon nanotube/graphene sandwiches: Facile catalytic growth on bifunctional natural catalysts and their applications as scaffolds for high-rate lithium-sulfur batteries, Adv. Mater. 26 (2014) 6100–6105. doi:10.1002/adma.201401243.

[37]C.F. Chen, A. Mistry, P.P. Mukherjee, Probing impedance and microstructure evolution in lithium-sulfur battery electrodes, J. Phys. Chem. C. 121 (2017) 21206–21216. doi:10.1021/acs.jpcc.7b07245.

[38] N.A. Cañas, K. Hirose, B. Pascucci, N. Wagner, K.A. Friedrich, R. Hiesgen, Investigations of lithium-sulfur batteries using electrochemical impedance spectroscopy, Electrochim. Acta. 97 (2013) 42–51. doi:10.1016/j.electacta.2013.02.101.

[39] S. Wei, L. Ma, K.E. Hendrickson, Z. Tu, L.A. Archer, Metal-Sulfur Battery Cathodes Based on PAN-Sulfur Composites, J. Am. Chem. Soc. 137 (2015) 12143–12152. doi:10.1021/jacs.5b08113.

[40] X. Liang, C. Hart, Q. Pang, A. Garsuch, T. Weiss, L.F. Nazar, A highly efficient polysulfide mediator for lithium-sulfur batteries, Nat. Commun. 6 (2015) 1–8. doi:10.1038/ncomms6682.

[41]T.Z. Hou, X. Chen, H.J. Peng, J.Q. Huang, B.Q. Li, Q. Zhang, B. Li, Design Principles for Heteroatom-Doped Nanocarbon to Achieve Strong Anchoring of Polysulfides for Lithium–Sulfur Batteries, Small. (2016) 3283–3291. doi:10.1002/smll.201600809.

[42] T.Z. Hou, H.J. Peng, J.Q. Huang, Q. Zhang, B. Li, The formation of strong-couple interactions between nitrogen-doped graphene and sulfur/lithium (poly)sulfides in lithium-sulfur batteries, 2D Mater. 2 (2015). doi:10.1088/2053-1583/2/1/014011.

[43]J.F. Moulder, W.F. Stickle, P.E. Sobol, K.D. Bomben, Handbook of X-ray photoelectron spectroscopy: a reference book of standard spectra for identification and interpretation of XPS data, Surf. Interface Anal. (1992) 261. doi:9780962702624.

CHAPTER 4

FUTURE WORK

In today's world, there is a growing demand for improved energy storage technology. Due to increasing global concerns regarding the reduction of fossil fuel usage, a strong emphasis is placed on utilizing clean and renewable energy sources. However, the intermittent nature of conventional renewable energy sources such as solar, wind and geothermal energy makes it necessary to develop reliable energy storage devices.

Lithium ion batteries have dominated the consumer electronics market for decades. Unfortunately, the conventional Lithium ion batteries are unable to meet the current demands of electric vehicles at a low cost. Therefore, we need to explore possibilities of next generation Lithium batteries such as Lithium-Sulfur, Lithium Air batteries etc.

In this thesis, we work on the improvement of Lithium Sulfur batteries. Lithium Sulfur batteries have several advantages over conventional Li-Ion batteries. Sulfur is cheap as it is abundantly available and also environmentally benign. Sulfur also has a high theoretical capacity of 1675 mAh/g and a volumetric energy density of 2600 Wh/kg. However, the complex electrochemistry behind the discharge and charge process contribute towards its disadvantages such as low coulumbic efficiency and fast capacity fading. Solubility of higher order polysulfides during the discharge process lead to polysulfide shuttling and loss of active material contributing to the cell's poor cycle performance.

In this thesis, we have combined the incorporation of mesoporous carbon, interlayers as a physical barrier and Nitrogen groups to improve polysulfide confinement and capacity retention. Despite obtaining an improved cell performance, the disadvantage of the system used was the utilization of thicker cathodes and interlayers which reduce the volumetric energy density. In order to move towards higher order Sulfur loading and move towards commercialization of Li-S batteries, it is important to consider these factors.

For future work, it would be worthwhile to consider improving on the concept of utilizing a Nitrogen Doped interlayer. Instead of incorporating a thick nanofiber interlayer, the carbon nanofiber mat can be grinded and directly deposited onto the separator or cathode by air-controlled electrospraying. The addition of Nitrogen groups to carbon nanofibers improves its dispersion capability and it can be uniformly deposited on to a separator, acting as a physical barrier to polysulfides.

Another future project to be explored is the combination of the N-doped carbon nanofibers produced from Urea as cathode and the cyclized PAN fiber as interlayer. It will be combining the effects of high nitrogen content and mesoporous carbon on polysulfide dissolution. In this project too, the elimination of a thick nanofiber mat and replacing it with a nanofiber surface coating on the separator to reduce the volumetric energy density.